SPE-200419-MS

A Critical Review of Capillary Number and its Application in Enhanced Oil Recovery

Hu Guo, China University of Petroleum-Beijing, Yan'an Universtiy and Universitat Stuttgart; Kaoping Song, China University of Petroleum-Beijing; Rudolf Hilfer, Universitat Stuttgart

This paper was prepared for presentation at the SPE Improved Oil Recovery Conference originally scheduled to be held in Tulsa, OK, USA, 18 – 22 April 2020. Due to COVID-19 the physical event was postponed until 31 August – 4 September 2020 and was changed to a virtual event. The official proceedings were published online on 30 August 2020.

Abstract

Capillary number (Ca), defined as dimensionless ratio of viscous force to capillary force, is one of the most important parameters in enhanced oil recovery (EOR). The ratio of viscous and capillary force is scale-dependent. At least 33 different Cas have been proposed, indicating inconsistencies between various applications and publications. The most concise definition containing velocity, interfacial tension and viscosity is most widely used in EOR. Many chemical EOR applications are thus based on the correlation between residual oil saturation (ROS) and Ca, which is also known as capillary desaturation curve (CDC). Various CDCs lead to a basic conclusion of using surfactant to reduce interfacial to ultra-low to get a minimum ROS and maximum displacement efficiency. However, after a deep analysis of Ca and recent new experimental observations, the traditional definition of Ca was found to have many limitations and based on misunderstandings. First, the basic object in EOR is a capillary-trapped oil ganglia thus Darcy's law is only valid under certain conditions. Further, many recent tests reported results contradicting previous ones. It seems most Cas cannot account for mixed-wet CDC. The influence of wettability on two-phase flow is important but not reflected in the definition of the Ca. Then, it is certainly very peculiar that, when the viscous and capillary forces acting on a blob are equal, the current most widely used classic Ca is equal to $2.2* 10^{-3}$. Ideally, the condition Ca ~ 1 marks the transition from capillary dominated to viscous-dominated flow, but most Cas cannot fulfill this expectation. These problems are caused by scale dependent flow characterization. It has been proved that the traditional Ca is of microscopic nature. Based on the dynamic characterization of the change of capillary force and viscous force in macroscopic scale, a macroscopic Ca can well explain these complex results. The requirement of ultra-low IFT from microscopic Ca for surfactant flood is not supported by macroscopic Ca. The effect of increasing water viscosity to EOR is much higher than reducing IFT. Realizing the microscopic nature of the traditional Ca and using CDCs based on the more reasonable macroscopic Ca helps to update screening criteria for chemical flooding.

Introduction

Enhanced oil recovery (EOR) involves how to extract original oil in place (OOIP) efficiently and economically[1,2], which has always been one of the hottest research interests for petroleum engineers, geologists, chemical engineers and sometimes physicists, chemists and hydrologists. The overall displacement efficiency of any oil recovery displacement process can be considered conveniently as the product of microscopic and macroscopic displacement efficiencies [1]. This is described by the formula,

$$E = E_D \cdot E_V \tag{1}$$

where E = overall displacement efficiency (oil recovered by process/oil in place at start of process), E_D = microscopic displacement efficiency (known as Displacement Efficiency) expressed as a fraction, and E_v = macroscopic (volumetric) displacement efficiency (known as Sweep Efficiency) expressed as a fraction.

The microscopic displacement efficiency depends on many factors, such as pore structure and distribution, microscopic heterogeneity, wettability and interfacial tension. E_D in Eq. (1) is reflected in the magnitude of residual oil saturation (ROS) in the region contacted by the displacing fluid[1]. It is generally believed that E_v is significantly affected by mobility ratio of the displacing phase and the displaced phase[2–4]. The most significant parameter to affect or determine the ROS is capillary number, which is defined as the ratio of viscous force to capillary force. Capillary forces are responsible, in part, for the inefficiency of the displacement of oil from petroleum reservoir during water flooding [5]. The capillary number (Ca) in close relation with capillary force is very important to characterize flow in porous media[6], because multiphase flow in porous media is constituted by the interplay of viscous and capillary forces[7]. Study of flow in core plugs in terms of Ca directly leads to the well accepted idea of addition of surfactants, such as surfactant-polymer flooding[8,9] and alkali-surfactant-polymer flooding[10,11], to injected brine to reduce oil/water interfacial tension (IFT) to ultra-low (10^{-3} mN/m) to get maximum oil recovery. The larger the Ca, the higher the oil recovery, especially for homogeneous reservoirs. However, many recent experimental and theoretical studies reported many phenomena that are hard to explain properly by classical Ca theory[12,13]. Even more important is the question whether surfactant-polymer (SP) flooding should replace alkali-surfactant-polymer (ASP) flooding as the development trend of chemical flooding, as many researchers contended[14–17]. This requires further investigation of the theoretical foundations of EOR, especially of Ca theory and mobility control theory.

Capillary number

It is now well accepted that the capillary number is a dimensionless group that quantifies the ratio of viscous force to capillary forces, as shown in Eq. (2).

$$\mathrm{Ca} = \frac{(viscous\,force)}{(capillary\,force)} \tag{2}$$

Although the first correlating group to establish the capillary number (Ca) was reported in 1927[18], the first clear definition of capillary number was described by Moore and Slobod in 1955[19] by using a concept of "Viscap" denoting viscosity and capillary pressure through a doublet model. The expressions Ca and Nc are frequently used to refer to capillary number. Ca is used in this paper for most cases.

The first clear correlating group definition is given in Eq. (3).

$$\mathrm{Ca} \equiv \frac{v\mu}{\sigma\cos\theta} \tag{3}$$

Where v is the Darcy velocity, μ is the viscosity of the displacing phase, σ is the interfacial tension (IFT) between wetting and non-wetting phase, and θ is the contact angle. As for system regardless of wettability (water wet, oil wet and intermediate wettability system), a viscous length group is given in Eq. (4).

$$L_{vis} \equiv \frac{v\mu L}{\sigma \cos\theta} \tag{4}$$

Where L_{vis} is the viscous length group, L is the distance over which capillary forces and viscous forces are competing (the length of doublet in the reference[19]). The only difference between Eq. (3) and (4) is the parameter length L. Perhaps due to the early interest in sandstone which is often water-wet, Eq. (3) is much more popular than Eq. (4). However, it is worth noticing that many people used Eq. (3) for oil wet system, which was not the original intention of the definition of Eq.(3). More importantly, Eq. (3) is dimensionless while Eq. (4) is not.

When cos θ is omitted, Eq. (3) becomes Eq. (5), which is the most widely used capillary number. For instance, in EOR textbook by Society of Petroleum Engineers (SPE) [1], the "capillary number is defined in Eq. (3) but without cos θ".

$$Ca \equiv \frac{v\mu}{\sigma} \tag{5}$$

The problem of finding suitable definitions for the capillary number is equal to the problem of finding precise and, if possible, concise characterizations for the viscous force and the capillary force. Lots of studies were devoted to this problem. According to our survey, at least 33 different capillary number definitions or correlating groups have been reported[19–25]. They are listed in Table 1. Capillary number in connection or combined with other scaling groups like the Bond number [26] and the trapping number[27,28] are not discussed here, although competition between gravity and capillary forces may affect oil recovery significantly [29]. Larson et al[18] summarized 14 correlating groups reported from 1927 to 1979 and Taber [5] summarized 17 correlating groups reported before 1979. The main difference between these capillary numbers is that some include the porosity while others include the relative permeability, or use different models to represent the absolutely permeability. For instance, a capillary number for a fracture is developed by using Eq. (5) and replacing the superficial (Darcy) velocity with the volumetric flow rate divided by the cross-sectional area[30]. The question is whether this substitute is physically sound and whether the use in some other circumstances meets the requirement of basic assumptions underlined in these mathematical models. Chatzis and Morrow[31] used three different scaling groups (Eq.(5), Eq.(6) and Eq. (7)) to investigate correlation of capillary number relationships for sandstone. The only difference in Eq.(6) and Eq.(7) is permeability to brine (k_w) or air (k_a). Although the capillary desaturation curve (CDC) looks similar when the Ca from Eq.(6) or Eq.(7) is used, the shape of CDC is quite different when comparing Eq.(5) and Eq.(6).

$$Ca \equiv \frac{k_w \Delta P}{L\sigma} \tag{6}$$

$$Ca \equiv \frac{k_a \Delta P}{L\sigma} \tag{7}$$

Table 1—Different capillary number expressions

No.	Year	Authors	Porous media	Capillary Number	Reference
1	1935	Fairbrother and Stubbs	Capillary	$\sqrt{\frac{v\mu}{\sigma}}$	[5]
2	1939	Leverett	Sandstone	$\frac{LP_c}{D\Delta P}$	[32]
3	1947	Brownell and Katz	Sandstone	$\frac{K\Delta P}{gL\sigma\cos\theta}$	[5]
4	1953	Ojeda, Preston and Calhoun	Sandstone	$\frac{\sigma}{\Delta P}$	[5]
5	1953	Ojeda, Preston and Calhoun	Sandstone	$\frac{k\Delta P}{L\sigma}$	[18]
6	1955	Moore and Slobod	Sandstone	$\frac{v\mu}{\sigma\cos\theta}$	[19]
7	1958	Saffman and Taylor	Hele—Shaw Cell	$\frac{v\mu}{\sigma}$	[33]
8	1969	Taber	Sandstone Berea	$\frac{\Delta P}{L\sigma}$	[34]
9	1973	Foster	Sandstone Berea	$\frac{u\mu}{\sigma\phi}$	[35]
10	1973	Lefebvre duPrey	Teflon, Steel, and Aluminum	$\frac{KK_{rw}\Delta P}{\phi L\sigma}$	[36]
11	1974	Melrose and Brandner	Unconsolidated Glass Beads	$\frac{KK_{rw}\Delta P}{dL\sigma}$	[37]
12	1974	Ehrlich, Hasiba and Raimondi	Sandstone	$\frac{K\Delta P}{\phi L\sigma}$	[38]
13	1975	Abrams	Sandstone Limestone	$\frac{v\mu_w}{\sigma}\left(\frac{\mu_w}{\mu_o}\right)^{0.4}$	[39]
14	1975	Abrams	Sandstone Limestone	$\frac{u\mu_w}{\sigma_{ow}\left[\phi\left(S_{oi}-S_{or}\right)\right]}$	[39]
15	1976	Dullien, MacDonald	Sandstone	$\frac{\overline{l}\Delta P}{\left(\frac{1}{D_e}-\frac{1}{D}\right)L\sigma}$	[40]
16	1977	Reed and Healy	Various	$\frac{K\Delta P}{\cos\theta L\sigma}$	[20]
17	1977	Stegemeier	Analysis of Various	$\frac{\phi N_{Le}^2 K_{rw}\psi}{2f}$	[41]
18	1978	Morrow	Teflon	$\frac{v\mu}{\sigma Z_{imb}\cos\theta}$	[5]
19	1979	Oh and Slattery	Model Pore	$\frac{\Delta P X_c}{\sigma}$	[42]
20	1979	Oh and Slattery	Pore model	$\frac{\nabla P k}{\sigma\varphi}$	[42]
21	1980	Arriola, Willhite and Green	Microcell	$\frac{\Delta P}{\sigma b_c}$	[22]
22	1984	Chatzis and Morrow	Sandstones	$\frac{k_w\Delta P}{L\sigma}$	[31]
23	1984	Chatzis and Morrow	Sandstones	$\frac{k_a\Delta P}{L\sigma}$	[31]
24	1987	Jiang Yanli	Sandstone	$\frac{KK_{rw}\cos\theta}{\Delta L}\cdot\left(\frac{1}{r_2}-\frac{1}{r_1}\right)$	[43]
25	1996	Hilfer	Analysis	$\frac{\mu_i\phi v_i L}{KP_b}, i=w, o$	[44]

No.	Year	Authors	Porous media	Capillary Number	Reference
26	2001	Hughes and Blunt	Numerical simulation	$\frac{Q\mu_w}{\overline{b}dN_y\sigma}$	[45]
27	2014	Rucker et al.	Sandstone	$\frac{l^{cl}}{r_p}\varphi\frac{v\mu}{\sigma}$	[7]
28	2011	Sheng	Analysis	$\frac{K\Delta P}{\phi L\sigma\cos\theta}$	[4]
29	2014	Armstrong et al.	Sintered glass	$\frac{l^{cl}{}_{\mu w}v^{Darcy}}{K^{rwpc}}$	[46]
30	2015	Hilfer, Armstrong, Berg, Georgiadis and Ott	Sample	$\frac{\mu_i\phi v_i L}{KK_i^r(S)P_C(S)}, i=o,w$	[47]
31	2017	Doorwar and Mohanty	Sandstones	$\left(\frac{v_w\mu_w}{\sigma_{ow}}\right)\left(\frac{\mu_o}{\mu_w}\right)^2\left(\frac{D^2}{K}\right)$	[48]
32	2018	AlQuaimi and Rossen	2D fractures	$\frac{\nabla PLgd_t}{2\sigma\left[1-\left(\frac{d_t}{d_b}\right)\right]\cos\theta}$	[30]
33	2019	Chang et al.	Micromodel	$\frac{4v\mu L}{\sigma\cos\theta}\left(\frac{1}{a}+\frac{1}{b}\right)$	[49]

Among the definitions of Ca in Table 1, the one proposed by Abrams[39] in 1975 is quite different from others because it incorporates the viscosity ratio, which is a key factor affecting the Sweep Efficiency E_v. This definition is shown in Eq. (8), where μ_w and μ_o denote water and oil viscosity respectively, v denotes water velocity. When the capillary number is combined with other scaling groups, a new capillary number can be obtained. For instance, the trapped number is derived from the capillary number and the Bond number. Doorwar and Motanty combined capillary number with the other dimensionless scaling group to get a new dimensionless scaling parameter, N_I, to predict recovery for unstable immiscible flows [48]. The scaling group, seen in Eq. (9), can be regarded as a capillary number or an extended capillary number because it is dimensionless and based on Eq. (4). In this paper, we regard all dimensionless scaling groups of the form in Eq. (2) or Eq. (3) as capillary number. Besides, Eq. (9) has similar form as Eq. (8) because they both involve a viscosity ratio term. However, they differ strongly in water-to-oil and oil-to-water viscosity ratio. In Eq. (9), D is diameter and K is permeability, σ_{ow} is IFT. However, the viscosity ratio is quite different.

$$\mathrm{Ca} \equiv \frac{v\mu_w}{\sigma}\left(\frac{\mu_w}{\mu_o}\right)^{0.4} \tag{8}$$

$$N_I \equiv \left(\frac{v_w\mu_w}{\sigma_{ow}}\right)\left(\frac{\mu_o}{\mu_w}\right)^2\left(\frac{D^2}{K}\right) \tag{9}$$

The above capillary numbers and those summarized in references[18] have different forms but are generally in shape of Eq. (3). However, based on macroscopic two-phase flow[50–58], one researcher [44,47,51,57,59] gave a definition of Ca quite different from previous ones:

$$Ca_i \equiv \frac{\mu_i v_i \phi L}{KP_b}, i=w,o \tag{10}$$

This Ca is defined as the ratio between the macroscopic viscous pressure drop and the macroscopic capillary pressure[59]. That is to say, the macroscopic capillary number conforms to Eq. (2) but capillary force and viscous force are characterized by macroscopic parameters rather than pore scale microscopic ones. Quite different from previous Ca expressions, this Ca [47] is a function of scale, saturation and velocity, and the definition involves the relative permeability, as is shown in Eq. (10) and Eq. (11). In other

words, as can be seen in Eq. (11), this Ca value is not a constant since relative permeability changes as saturation changes. This captures the dynamic force change during two-phase flow.

$$F_i(S, v_i, L) \equiv \frac{\text{(viscous pressure drop in phase i)}}{\text{capillary pressure}} = \frac{\mu_i \phi v_i L}{K K_i^r(S) P_c(S)} \tag{11}$$

By using fracture permeability model, a new Ca for a fracture is given [45] in Eq. (12).

$$\text{Ca} \equiv \frac{\nabla P L_g d_t}{2\sigma\left[1-\left(\frac{d_t}{d_b}\right)\right]\cos\theta} \tag{12}$$

AlQuaimi and Rossen[30] improved this fracture model by incorporating fracturing permeability

$$\text{Ca} \equiv \frac{\nabla P k_f}{\sigma\cos\theta}\left[\left(\frac{12}{2}\right)\left(\frac{d_t}{d_b}\right)\left(\frac{L_g}{d_t}\right)\left(\frac{1}{1-\left(\frac{d_t}{d_b}\right)}\right)\right] \tag{13}$$

This Ca was found better in natural fractured media, as is shown in Eq. (13). Hence, Cas have been proposed for matrix-pore system and matrix-fracture system.

Summary

1. Up to present, 33 different capillary number expressing have been put forward.
2. These Cas fall into two big group: macroscopic Ca and microscopic Ca.
3. Most Cas are proposed for pore-matrix system and some for fracture-matrix system.
4. Some contain a wettability factor, others not.
5. Some contain permeability and relative permeability factors.
6. Some Cas were believed to be equivalent to each other, their conditions remained to be checked.
7. Only two Cas incorporate the viscosity ratio, but in a quite different pattern.
8. Serverals new definitions for Ca were proposed recently, indicating that Ca theory still needs to be improved further.

Classic Capillary Desaturation Curves

The capillary number is frequently used to create capillary desaturation curves (CDC), which describe the quantitative correlations between residual phase saturation (wetting or non-wetting) and the value of the capillary number. CDC has important application in EOR since the core issue in EOR is to reduce residual oil saturation (ROS) significantly and economically. CDC is one of the most important curves in EOR[60]. Typical CDCs are obtained by varying the Ca parameters in the same core or model. The process to obtain such CDCs was well introduced in references [47,51]. Because it is difficult to reuse the same core for multiple tests, frequently different cores with similar feature are used to correlate ROS and Ca to get a CDC. The scattering of test results reflected the correlationship as well as the difference in models. Even when based on different definitions, many CDC are similar. Abrams [39]rewrote the test results of Moore and Slobod [19], as seen in Figure 1 [39]. The ratio of the viscosities of the displacing and displaced phase is close to 1. Note the ordinate is oil saturation at breakthrough. Abrams conducted several tests with sandstone cores and one with limestone. The result is given in Figure 2[39]. In Figure 2, the solid line represents limestone core flooding. Please note that the viscosity ratio is incorporated into the Ca and the velocity is also different from others[39].

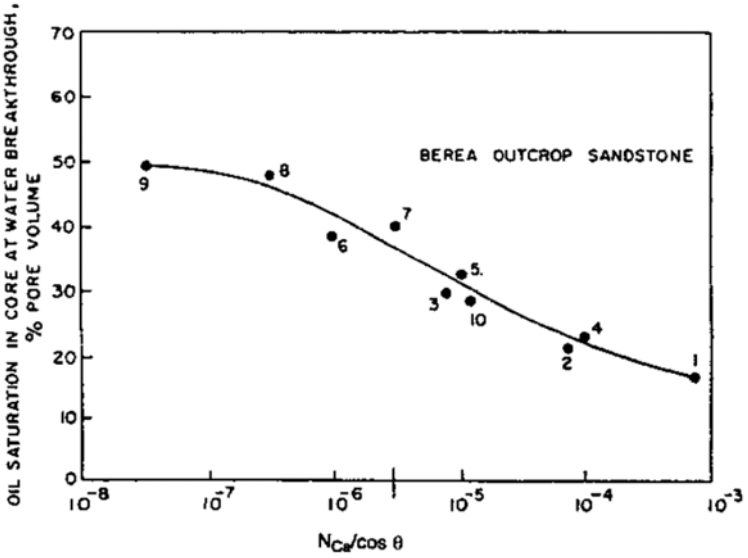

Figure 1—Moore and Slobod CDC [39]

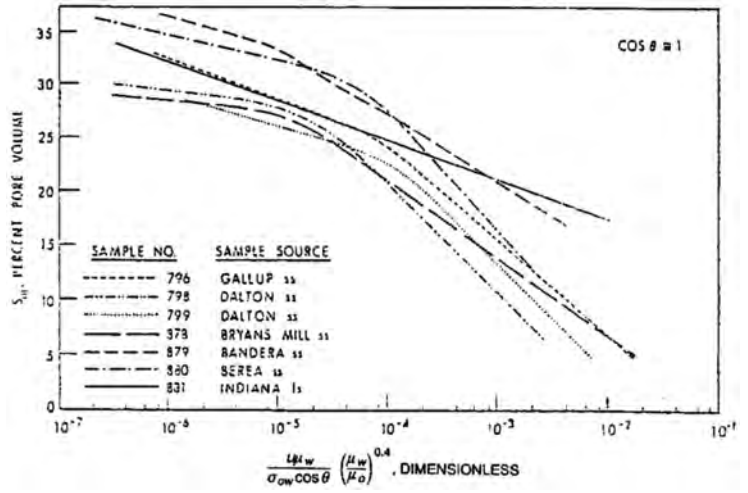

Figure 2—Abrams CDC [39]

Figure 3 summarizes several CDC test results [41]. In Figure 3, the two dashed curves show the nonwetting phase ROS, while the solid curves show the ROS of wetting phase. Many researchers [39,40] reported tests for wettability affected CDC. A stark contrast between between the non-wetting and wetting phase was visible. The CDC for the wetting phase, like oil in oil-wet carbonate rock, was visibly more gradual [61]. Typical CDCs for the wetting and non-wetting phases are shown in Figure 4 from [2]. Sandstone reservoirs and carbonate reservoirs were often regarded as water-wet and oil-wet respectively, although some researchers believed they were mixed-wet. The capillary number was about one order of magnitude higher under oil-wet conditions in comparison to water-wet conditions[62].

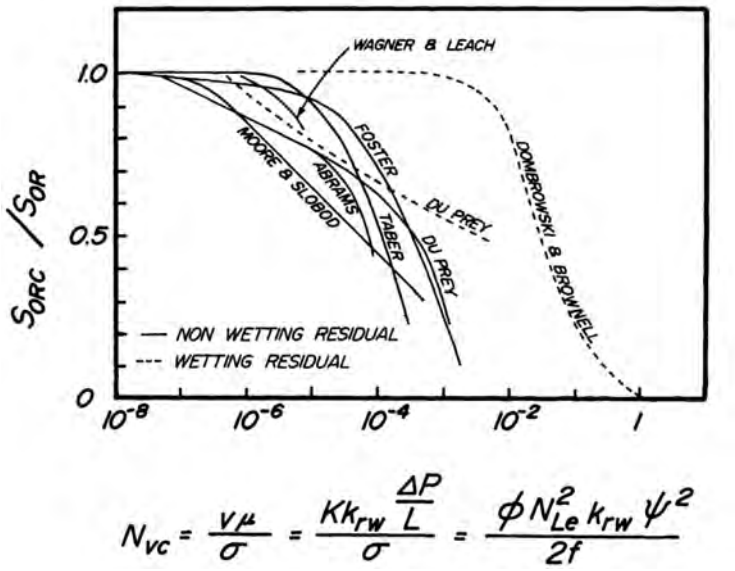

Figure 3—Typical CDCs [41]

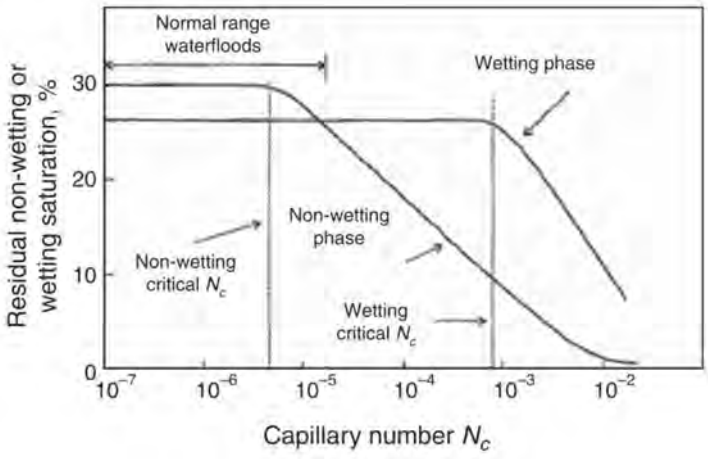

Figure 4—Wettability affected CDC

The ease to displace continuous and discontinuous residual oil within the same core sample is shown in Figure 5 [63]. The value of Ca that is required to reduce the ROS of an initially disconnected fluid to a particular value is several times higher, for instance, 5 times, than that required to reduce the ROS of an initially connected fluid to the same value[31,63]. Sheng provided water, oil and emulsion phase CDCs, as shown in Figure 6 [3].

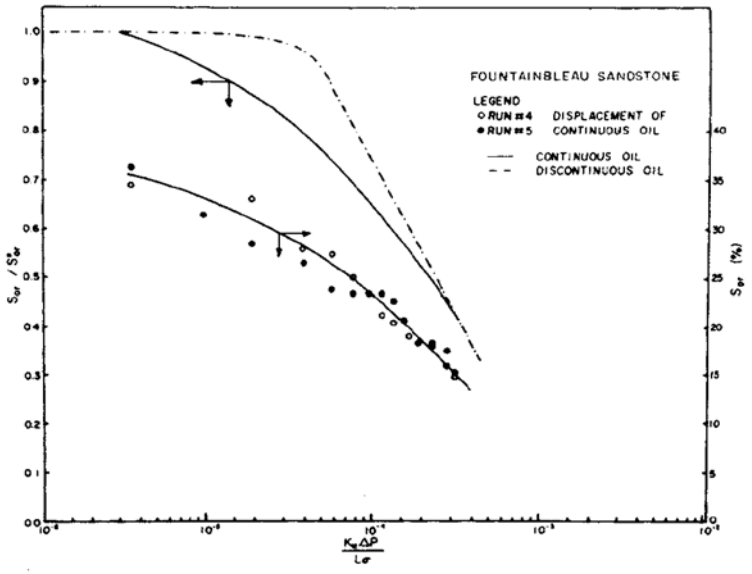

Figure 5—CDC comparison of continuous and discontinuous oil [31]

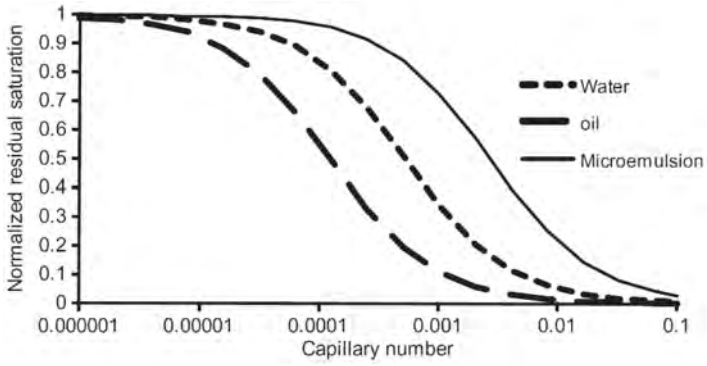

Figure 6—Microemulsion CDC [3]

The above mentioned CDCs are regarded as classic because they were all based on similar Cas, such as Eq.(5), Eq.(6) and Eq.(7), and had many common features.

1. The larger the Ca, the lower the ROS. A maximum oil recovery thus requires a maximum Ca.
2. When Ca reaches 10^{-3} to 10^{-2} [31,63], the mobilization of residual oil is complete. In other words, all ROSs go to zero in the end. However, Ca values higher than 10^{-2} were rarely reported.
3. Most CDCs have obvious critical Ca values (Cac). When the Ca value goes higher than Cac, ROS drops quickly as Ca increases further. Before Cac, ROS does not change obviously as Ca increases. For most porous media, a value of Cac between 10^{-6} and 10^{-5} correspondes to the beginning of mobilization[63].
4. Oil-wet and water-wet rock CDC behaves differently. Cac for wetting phase is one [62] or two[2] orders of magnitude higher than non-wetting phase.
5. Mixed-wet CDCs[64–66] are different from that of water-wet and oil-wet.
6. Ease of displacement of continuous and discontinuous oil is different.
7. The permeability of most Berea sandstones used for CDC tests is between 40 and 2500 mD[31], except for one limestone of 26 mD [39]and two Bandera sandstones of 10mD[19] and 32 mD[39].

Classic CDCs have important applications in EOR. Ca is one of the most important parameters in affecting

E_D in Eq.(1). To reduce the ROS, capillary number should be large enough to exceed a critical Ca value. High values can be attained by reducing the IFT to an ultra-low level, or by increasing the displacing viscosity since the velocity can hardly be increased under reservoir conditions. Among different EOR techniques, chemical flooding is more closely related with the capillary number[1,2]. Surfactant is thus required to reduce the oil/water IFT from around typical 35 mN/m to 10^{-3} mN/m to get maximum capillary number [10,11,67]. This is well accepted by many, if not all, petroleum engineers. Classic CDCs also imply that the contribution of the increasing displacing phase viscosity is the same to reducing IFT to the same order of magnitude when the value of capillary number is the same. In other words, it was not the viscosity or the IFT but capillary number that determined the ROS. However, this is not in agreement with many laboratory tests[68–72] and current chemical flooding practice[12,13].

New CDCs

It should be noted that the CDC is closely related with the definition of Ca. As is shown in Table 1, there are 33 different definitions of Ca. Interestingly, Chatzis and Morrow [31]reported different CDCs based on the same core flooding tests with different expressions of Ca. In their publication, Eq.(5), Eq.(6), and Eq. (7) were all used. The CDC trends and shapes are different. Although they concluded that caution must be exercised when applying these CDCs to porous media of distinctly different pore structure and to tertiary oil recovery[31], which one of these three expressions is the best to describe the CDC remained unknown. Many different CDCs have been given recently.

Qi et al [73] reported a CDC (Figure 7) quite different from classic ones. After checking the test condition, it is found that the two-dimensional three-layer long cores (4cm*4cm*30cm) used for Figure 7 were quite different from typical cores used in classic CDC tests. The same physical model used was well shown in reference[70]. In addition, the velocity also differs to other tests although the Eq. (5) is used. Note in this figure the dots are not from one core, but from different cores. It is interesting that the ROS is not further reduced when Ca goes higher than 10^{-2}. In addition, the minimum ROS does not go to zero. The Ca values in their tests went high to 10^{-1}, which were rarely reported. However, the ROS in Figure 7 is not the actual residual oil saturation but remaining oil saturation due to insufficient sweep efficiency.

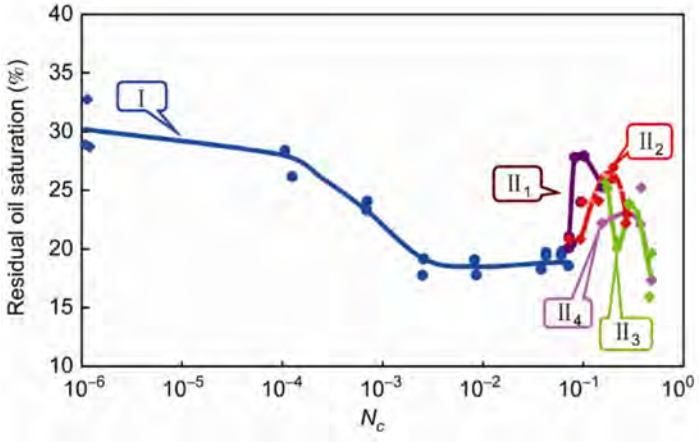

Figure 7—A different CDC[73]

Wang et. al. reported a polymer flooding CDC, seen in Figure 8[74]. In this figure, the upper group referred to Oil Recovery Factor while the lower group referred to the Residual Oil Saturation. They believed that viscoelasticity of a HPAM polymer could play an important role in reducing ROS, which is not reported in classic CDCs. Other researchers also believe that viscoelasticity could reduce the ROS[75–78]. According to the classic CDCs, polymers play a limited or no role in reducing the ROS because it can increase the

brine viscosity to at most 2 order of magnitude due to the reservoir pressure gradient constraint. In other words, the polymer itself cannot increase Ca value to Cac [1]. Therefore, it does not reduce ROS[79].

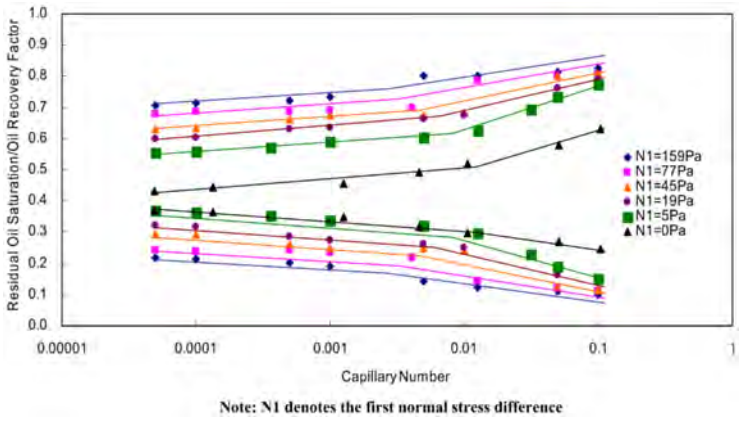

Figure 8—Viscoelasticity affected CDC[74]

Qi et. al. reported a quite different polymer flooding CDC in which the polymer without addition of surfactant can reduce the ROS to almost zero, as is shown in Figure 9 [80]. They also attributed this to the viscoelasticity effect of HPAM to the ROS[81]. However, the extremely low ROS in their tests may be more caused by the gravity-stable effect rather than the viscoelasticity effect of HPAM because their cores were vertically placed. For typical chemical flooding tests, the cores were horizontally placed to exclude the gravity effect to oil recovery. In another vertically placed flood test[82], gravity-stable surfactant flooding without addition of the polymer to control mobility achieved a very high recovery, which was never reported or proven impossible for horizontally placed core floods and field tests. In addition, this CDC (Figure 9) was obtained in a secondary recovery model at high initial oil saturation where oil was continuous. However, some cores were vertically placed to get CDCs, while others were horizontally placed. Most core flooding tests in China were conducted in a horizontal manner.

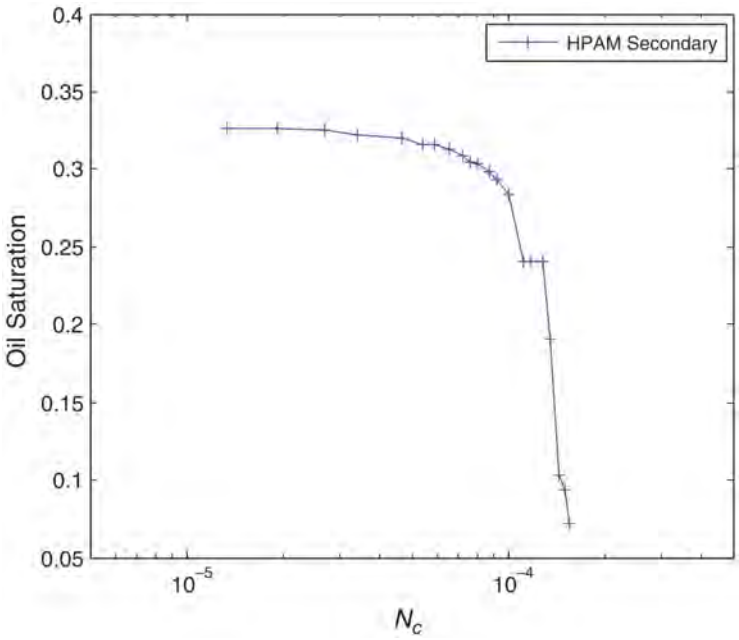

Figure 9—A different HPAM CDC [80]

Mai et. al.[83,84] reported a flow rate effect on heavy oil water flooding. They found that the breakthrough oil recovery decreased with the increase of Ca defined in Eq. (8). Doorwar and Mohanty[48] also reported polymer flooding viscous oil test results which are quite different from classic CDC conclusions. Figure 10 (a) and (b) are a summary of polymer displacing very viscous oil under water-wet rock conditions. Figure 10 (a) indicates that oil recovery correlates poorly with the Ca defined in Eq. (2). However, after combining an oil-to-water viscosity ratio and the Ca, the recovery correlates well with this new scaling group, as shown in Figure 10(b). Since this new group is dimensionless and based on Eq.(2), we still regard N_I as a capillary number, as shown in Eq.(9). Their results are also not in agreement with the classic CDCs in which a higher Ca leads to a higher recovery. The CDC from a viscous oil flooding test[66] in mixed-wet rocks also behaves differently from typical CDCs.

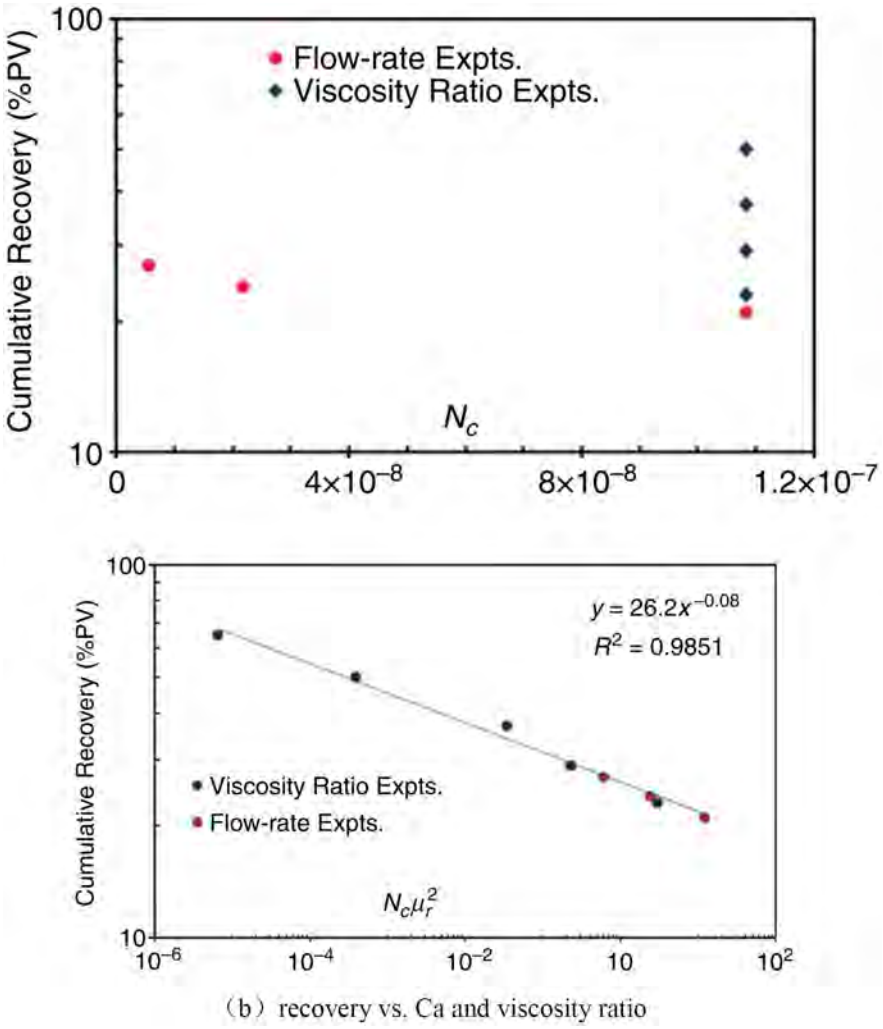

Figure 10—Cumulative recovery correlation with Ca [48]

Although the wettability effect on the CDC has been studied[64], their results differ regarding the shape of the wetting-phase (like water displacing oil in oil-wet rock). The typical wetting-phase CDCs in Figure 4 and Figure 6 have a Cac, while the CDCs for oil-wet and mixed-wet rocks [39,64,66,85] are more gradual without such a Cac. Figure 11 [66] and Figure 12 [85] show this difference. In Figure 11, the oil in core 2 is viscous (viscosity of 320 cP). While in Figure 12, the major difference between these three CDCs is the IFT which is one order of magnitude lower from each other. Since the cores used in Figure 12 are not significantly different, it is strange that these CDCs went apart from each other. The capillary end effect was believed one major cause for this atypical CDC, although long cores (30 cm) have been used in these

tests. The ROS for a mixed-wet rock was not regarded as real ROS but as remaining oil saturation[85]. Han et. al.[61] also reported a gradual desaturation curve for an oil-wet carbonate rock, which was horizontal placed in their tests.

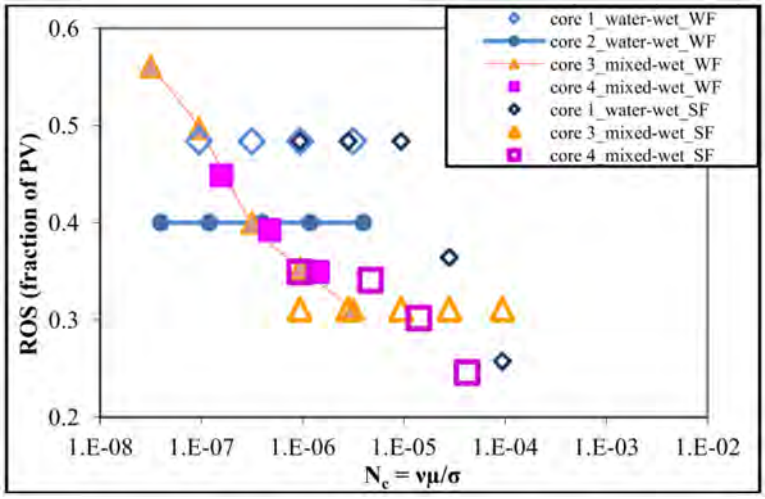

Figure 11—Mixed-wet rock CDC [66]

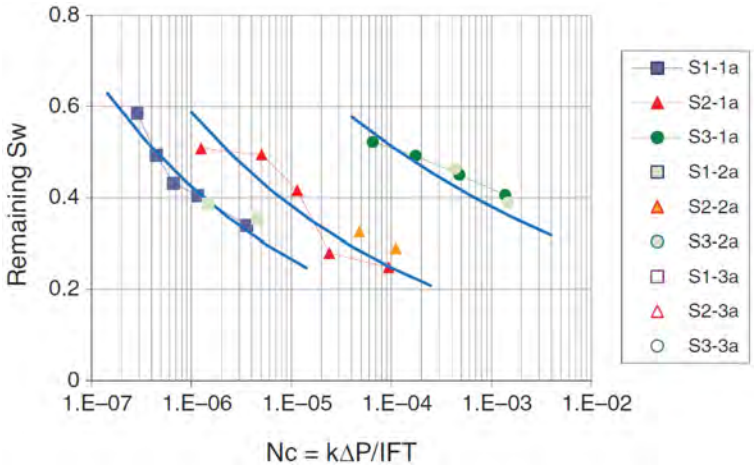

Figure 12—Atypical wetting phase CDC[85]

AlQuaimi and Rossen [30] proposed a new capillary-number definition for fractures that incorporated geometrical characterization of the fracture, as shown in Eq.(13). It is called fracture capillary number in this paper. It seems that the CDC based on their revised definition scatter less than the curves obtained for the conventional definition of the Ca. In addition, their revised Ca values are much higher than the conventional Ca and their largest Ca values approach unity. It is worth mentioning that the models used for the CDC are different to the cores used for a typical CDC.

Chang et al[49] used a complete capillary number (No.33 in Table 1) by adding pore-scale characteristics (pore-throat diameter and micromodel depth) to study unstable drainage of brine by supercritical CO2. The most special observation of their experiment results is the non-monotonic increase of the CO2 saturation to capillary number increase. This capillary saturation is opposite process of capillary desaturation. Although transition from capillary fingering to viscous fingering during the instable drainage process may help to account for their test results, the correlation between saturation and capillary number is quite inconsistent with previous studies [86]. After all, a non-monotonic saturation change with the Ca was not reported.

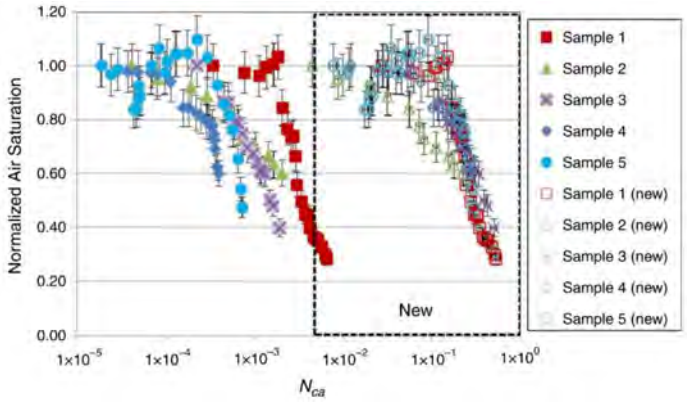

Figure 13—CDC with new Ca[30]

In reference [51] a CDC based on the macroscopic capillary number proposed in [44] was shown for the first time. Reference[51] discussed trapping and mobilization in continuous and discontinuous displacement and proposed a length parameter to distinguish them. It used the experimental data in other references and gave a more reasonable CDC as shown in Figure 14 [51]. In this figure, the Ca with a top line is the macroscopic capillary number. The macroscopic Ca values which go close to unity are much higher than microscopic ones. Although it has a similar shape with the CDC using the same parameters, it is the first CDC using macroscopic capillary number in Eq.(10). Note that the breaking point for continuous mode displacement occurs around 1 in Figure 14.

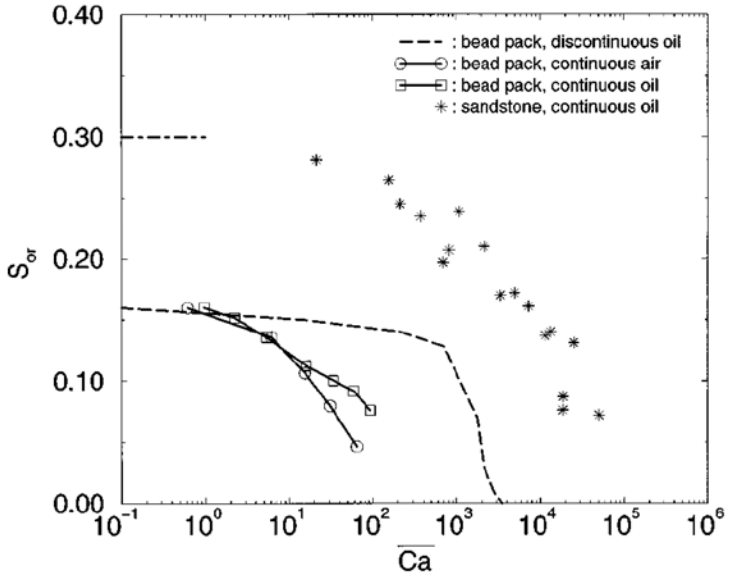

Figure 14—CDC based on macroscopic capillary number [51]

Armstrong et. al. [46] modified the macroscopic capillary number definition [44] and gave a new capillary number (No.30 in Table 1). They used an average cluster length l^{cl} (seen in Figure 15[46]) and created a CDC different from all previous ones. Figure 15 shows a different CDC based on different Cas. The shape of the CDC is very interesting since the ROS drastically decreases after the Ca goes to a certain value. Note the right angle in the modified CDC.

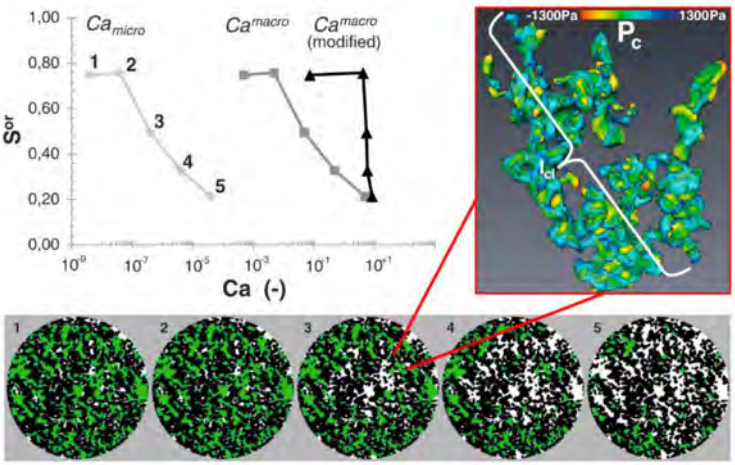

Figure 15—CDC with improved Ca [46]

In reference [47] a theoretical CDC was shown which differs from all the other previous ones, as seen in Figure 16. They also build a connection between the macroscopic Ca and the microscopic Ca. In Figure 16, logarithmic coordinate is used. There was a minimum ROS that does not appear in the CDC in Figure 15. This seems much more reasonable since it reflects a basic observation that the immiscible oil recovery seldom goes to 100%. The maximum Ca values in this figure are approaching unity. Since so many different CDC were reported, one question arises: why are there so many different Cas and CDCs?

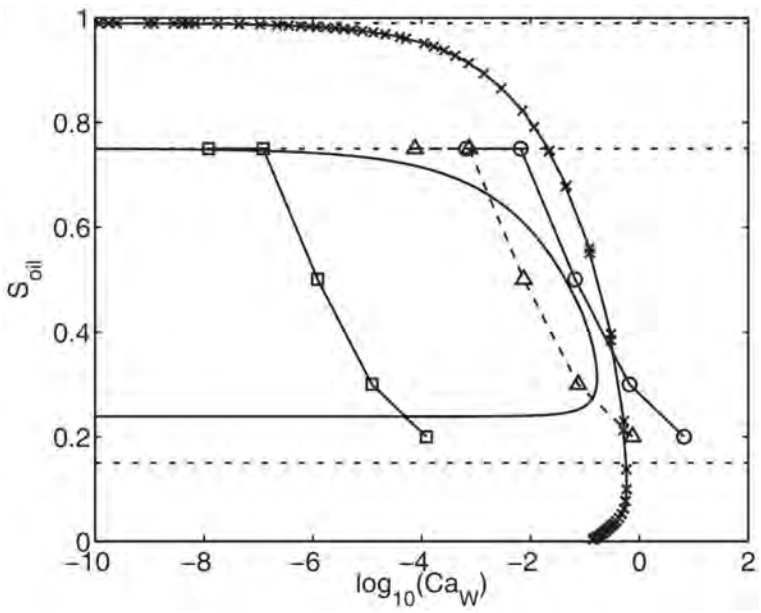

Figure 16—Two theoretical CDCs[47]

Physical nature

Since the Ca has been widely used in characterization of forces interplay, its physical nature is thus important. It is generally accepted that the capillary number is the ratio of viscous force to capillary force in porous media, the key is thus how to characterize them. The flow in porous media is found scale dependent[87]. At small scale, the flow is capillary dominated while at large scale it is viscous dominated, as is shown in Figure 17 [87]. The intermediate scale between small scale and large scale is capillary-viscous coupling which is one of the most difficult problems in upscaling. Lenormand et al[86] regarded the flow in porous media as characterized by capillary number defined in Eq.(5) and viscosity ratio. They

used numerical simulations and experiments performed in homogeneous transparent etched networks and proposed three basic flow regimes: viscous fingering, capillary fingering and stable displacement. Their typical results are shown in Figure 18[86]. When the Ca defined in Eq.(5) approachs unity, the saturation or desaturation is affected by the viscosity ratio. Flow regime transmited from viscous fingering to stable displacement as indicated by Figure 18. It remains unknown where the scale lies and whether capillary fingering disappear when Ca is high.

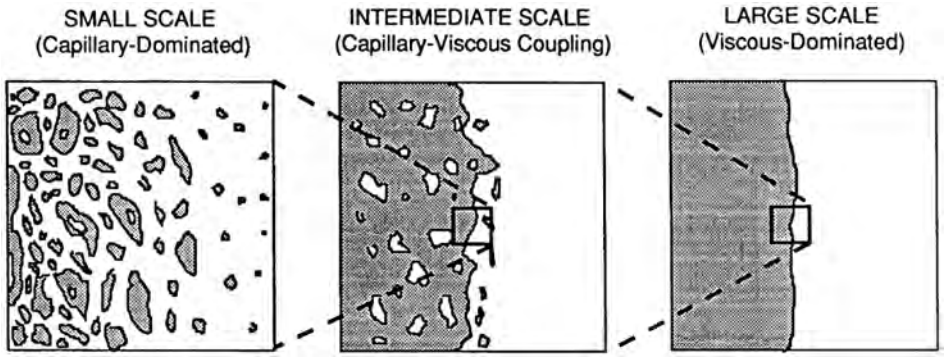

Figure 17—The scale-dependence of force balance[87]

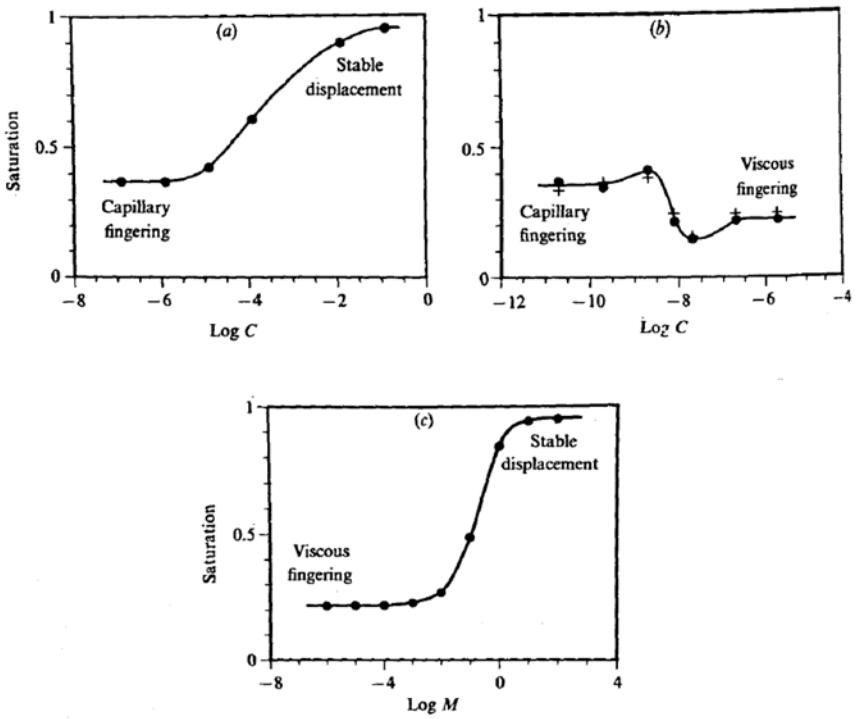

Figure 18—Flow regimes characterized by capillary number C and viscosity ratio M[86]: (a) log M=1.9, (b) logM=-4.7, (c), logC=0

Rucker et al[7] also noticed the problem between the pore-scale and the Darcy-scale and proposed an intermediate scale flow regime between those scales. Flow regimes change from connected pathways to disconnected ones is well shown in Figure 19[7]. Figure 20[88] shows the difference between the microscale and the macroscale in a typical numerical simulation model. Obviously, many parameters that are different on the microscale disappear on macroscopic scales. A more common concept of the scale-dependent representative elementary volume (REV) widely used in many areas is given in Figure 21[6]. If the scale is too small, such as the typical pore-scale, the upscaling process is misleading because the

characteristic parameters are not representative[89]. This is especially true for porous media that are mostly heterogeneous.

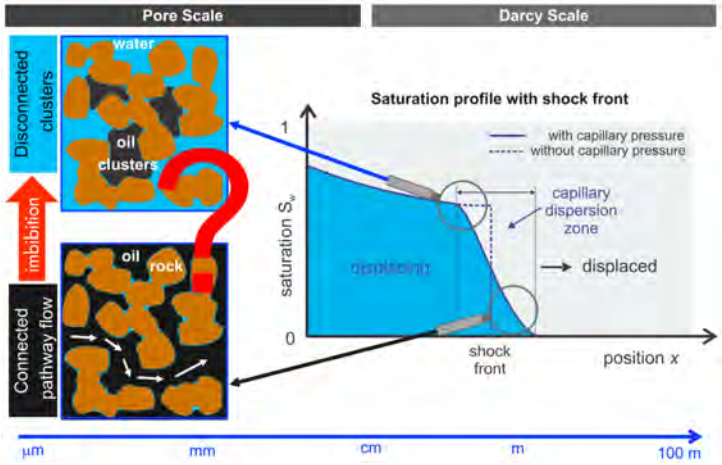

Figure 19—Pore-scale and Darcy-scale[7]

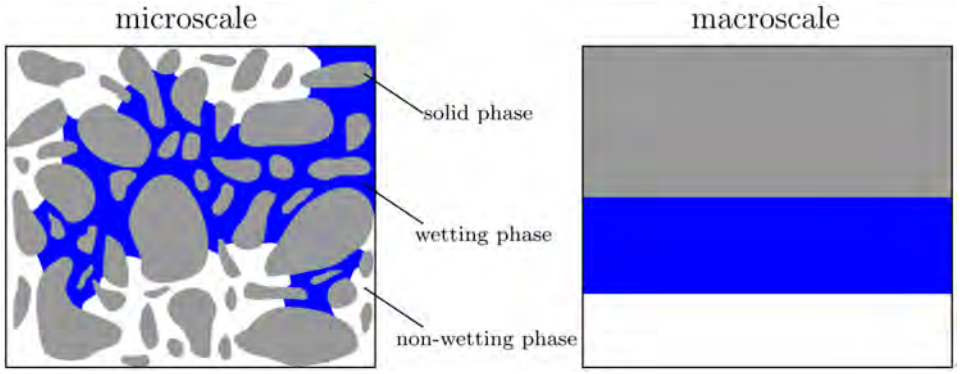

Figure 20—Scale difference in numerical simulation[88]

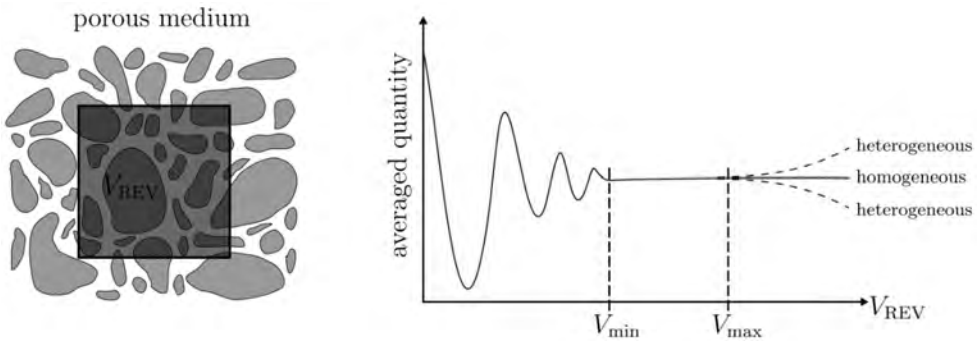

Figure 21—Representative elementary volume (REV)[6]

Heterogeneity itself is scale-dependent in physical nature[54]. This is well reflected in the recent publication [90], where differential porosities and permeabilities were introduced to reflect scale- dependent information on geometry fluctuations in permeability and porosity. Their study well showed how homogeneity can be deceptive without high-precision analysis for REV studies. The upscaling from the pore scale to a larger scale requires careful attention to the physical nature of heterogeneity [54,55,91,92], although some progress has been made recently[46,90,93–95]. In short, the differences in the definition of

the capillary number and CDC are caused by scale and heterogeneity, although heterogeneity can be both microscopic and macroscopic.

Figure 22 eloborates a possible classification of capillary number with respect to different scales: microscopic scale, macroscopic and mesoscopic scale. The macroscopic scale can be the Darcy scale, which is easy to understand for engineering considerations. The macroscopic scale meets the requirement of REV in most cases and is characterized by macroscopic parameters like permeability and porosity. The microscopic scale is the pore scale with one or several pores. The macroscopic parameters cannot be applied to the microscopic scale directly unless it is homogeneous from an engineering perspective, even though the homogeneity depends on precision[90]. The criteria to distinguish the microscopic scale and macroscopic in this paper depends on the engineering goal. To make it simple, we regard the scale that can be directly seen or easily measured without special technique as macroscopic. Thus, reservoirs cores that are cm long are regarded as macroscopic. Pores that have a dimension of micron (pm) are generally regarded as microscopic scale. The range between the macroscopic and the microscopic scale is the mesoscale.

$$C_a = \frac{(viscous\ force)}{(capillary\ force)} = \frac{F_v}{F_c}$$

Figure 22—Scale-dependence of Ca

As far as the capillary number is concerned, it only is physically meaningful if the capillary force and viscous force are on the same scale. Thus, when the capillary force and the viscous force are both characterized by the macroscopic scale like Darcy's law, the ratio is macroscopic Ca (MaCa). Similarly, when the both capillary force and viscous force are characterized by microscopic parameters, its ratio is microscopic Ca (MiCa). If one force is microscopic while the other is macroscopic, its ratio is called mesoscale capillary number (MeCa). By this classification, it sounds more reasonable to explain the various Ca expressions and CDCs. Many researchers noticed the problems of the Ca[46,47,50,59,95,96]. For instance, the critical capillary number marks the point where the viscous force begins to dominate the capillary force[59]. Surprisingly, all experimentally observed values for the Cac are much smaller than one[25,31,63,64,97]. It is certainly peculiar that when the viscous and the capillary forces acting on a blob are equal the capillary number that is supposed to be equal to the ratio of viscous-to-capillary forces is equal to 2.2* 10^{-3} [98]. Chatzis and Morrow[31] used so-called equivalent Ca expressions [18] in their tests and showed quite different CDCs which they did not explain properly. Besides, almost all values of the Ca in literatures are so small (10^{-7} to 10^{-3}) and it is strange why effective oil mobilization has happened at such small capillary numbers even for trapped oil. Thus, the microscopic scale nature [44,46,47,59,89] of most widely used Cas is pointed out but was not widely recognized.

MiCa

As discussed in many publications[44,46,47,59,89], most of the Cas in Table 1 are actually microscopic, which is based on discontinuous trapped ganglia in pores. The capillary number defined in Eq. (5) is thus called MiCa according to Figure 22. At the microscopic pore scale, pathway flow and film swelling[99], cooperate pore filling[100,101], snap-off [7,102,103], droplet fragmentation[104], no breaking-up mobilization[105], coalescence[95], corner flow[99,100] as well as Haines jumps[7,106,107]

are main flow mechanisms. These pore-scale flow behaviors are not characterized by Darcy's law[44]. The average low flow rate cannot reflect the high phase velocity in individual pores[7], hence the frequently used velocity or Darcy velocity in many publications is at most an estimation. It should be noted that MiCa does not involve the Sweep Efficiency because it is a microscopic concept or the Sweep Efficiency is assumed one. In many experiments, microscopic displacement efficiency [37,108] is calculated from core flooding tests. This is weird because it is not microscopic at all. More importantly, the in situ contact angle in Eq.(3) used in micrsocopic capillary number may be different from the one tested from the surface[109,110]. The present way of calculating the capillary pressure by the Young-Laplace equation should be used with caution because the microscopic lengths [31,111] or the characteristic lengths [63,86] vary with respect to the pore geometry. For homogeneous models, the IFT and microscopic lengths may be uniform. The average pore diameter from the mercury injection experiment cannot represent the complex pore distribution especially for low permeability rocks. Except for some very homogeneous models, the various capillary numbers based on Eq.(5) can be more regarded as qualitative rather than quantitative. Many high permeability cores were homogeneous within the scope of EOR, while low permeability cores were more heterogeneous. The combination of the macroscopic Darcy velocity with the MiCa is meaningless except for very homogeneous porous media. The connection between homogeneous models in forms of Eq.(5) and Eq.(6) remains to be further investigated, although their difference in physics has been well studied[44]. It is worthwhile to note that although the "macroscopic capillary number" is used in references[100,112], the Ca in these references is actually microscopic. Since the models used are very homogeneous from the EOR perspective, their conclusions may be less affected.

MaCa

By using typical well accepted macroscopic parameters [44] like permeability, relative permeability, porosity and capillary pressure[50,58], the MaCa in form of Eq.(10)[47,59] and its improvement[7,46] can well reflect the relative domination of the macroscopic capillary force and the viscous force in two- phase flow in porous media. The important IFT parameter in all previous Cas (MiCa) is not used in the MaCa due to the fact that no rigorous connection between microscopic Newton and Laplace law and the macroscopic generalized Darcy law exists[47]. A capillary breakthrough pressure which reflected the importance of microscopic wetting properties and flow mechanism on the macroscale was used in MaCa[44,59]. The well-defined capillary breakthrough pressure[59] or average capillary pressure[46] was more complex than the IFT parameter which can be easily tested outside a porous medium. Thus it is better to be used as a quantitative characterization possibility rather than certainty because the macroscopic quantity defined in Eq.(11) indicates that macroscopic capillary number is actually a function of many parameters. For instance, relative permeability is found to depend on saturation, changes of saturation, residual saturations, interfacial area and wetting properties[50,51]. Capillary force between oil and water phase may disappear in some place or some stage. In addition, the saturation in Eq. (11) can be remaining oil saturation rather than the ROS. Macroscopic capillary number theory helps to overcome the improper assumption [59] and can explain many phenomena better than the microscopic capillary number. For instance, ideally *Ca#1* represents the transition from capillary-dominated to viscous-dominated flow [47], while many previous Cas do not meet this idea. For many heterogeneous porous media, how to make the displacing phase arrive at the trapped oil ganglia in different pores is a key problem in EOR, however, a full sweep is a basic assumption in the MiCa. For the MaCa, the contact can be reflected by saturation and length parameter. The relative contribution of the viscous force and the capillary force determines whether the displaced phase can be mobilized. One important application of the MaCa is to analyze the dynamic force in combination with other macroscopic scaling groups like macroscopic gravity number[44,59]. The MaCa can better account for the various chemical flooding tests. The direct parameter viscosity is more important than the indirect parameter IFT which affects capillary breakthrough pressure. The MaCa can also help to reflect the IFT dependence

on permeability[59]. For high permeability rocks, the necessity to reduce IFT is not urgent because MaCa can be higher than unity even without ultra-low IFT. As for low permeability rocks, the surfactant will be adsorbed which can be reflected by the relative permeability and the capillary breakthrough pressure. This makes the ultra-low IFT effect much discounted. Thus, only for medium permeability rocks, the ultra-low IFT may contribute significantly to the high oil recovery. Hence, the necessity of reducing the IFT to ultra-low to achieve maximum oil recovery for most reservoirs is worth investigating. Many chemical flooding tests[11,12,113] indicate that the contribution of the mobility control is higher than the reduction of IFT. More importantly, the important role of interfacial viscoelaticity on residual oil recovery[114–119] cannot be well reflected in classic CDC and MiCa but be possible involved in macroscopic capillary number parameters. This needs further investigation.

MeCa

The flow transition from the microscopic pore scale to the macroscopic Darcy scale involves a significant change in flow regimes [7]. Unitl today there seems to be no rigorous connection between the microscopic Newton law, the Laplace law and the macroscopic generalized Darcy law[47]. Thus a modified capillary number containing the macroscopic parameter porosity, and microscopic parameters, like velocity, interfacial tension and viscosity, and other parameters, like an average cluster length and pore throat radius, is given[46]. This Ca is called macroscopic Ca[7]. However, the combination of macroscopic and microscopic parameters makes it hard to judge whether it is macroscopic as it is contended. More importantly, this practice leads to the strange conclusion that the pore scale capillary number is a function of the saturation[47]. The difference in physical nature between microscopc and macroscopic scale, such as constitutive laws, has been well discussed [44,47,53,54,56,59]. Considering the fact that Eq.(5) is actually microscopic, the Ca in reference[46] is more microscopic if it would not contain the cluster length which is either microscopic or macroscopic. Thus, the Ca proposed by Armstrong[46] can be called mesoscopic capillary number MeCa which contains parameters between microscopic and macroscopic scales. In order to reflect the ease of flow in connected pathways as well as mechanism of ganglion dynamics in inter-pores [7], a MeCa C_a^e is proposed in Eq.(14). Different from the Ca given by Armstrong[46], porosity is not included and connected ganglia length l_{co} replaced cluster length l^{cl}. Some researchers also attempted to set up a connection between macroscopic pressure gradient and MiCa by using a critical ganglia length[60] or a largest ganglia length[105]. The average pore radius is used instead of a pore-throat or a pore radius in reference[30]. This mesoscopic Ca helps to bridge the pore scale and Darcy scale flow and can reflect the fact that it is much easier to displace connected oil clusters than disconnected oil clusters. The value of the MeCa can be much higher than the MiCa. The MeCa for continuous oil clusters is much larger than for discontinuous oil clusters. However, a constitutive law for the mesoscale remaines to be developed yet [47].

$$C_a^e \equiv \frac{l_{co}}{d}\frac{v\mu}{\sigma} \tag{14}$$

Where, l_{co}=connected oil ganglia, d =average pore radius.

New observations

Rabbani et al[101] reported very interesting test results which cannot be well explained by previous Ca theory. In their tests, the flow behavior is not more affected by pore size gradient than capillary number defined in Eq.(5) (MiCa). At the same MiCa, flow behavior differs greatly. Gradual and monotonic variation of pore sizes along the front path suppresses viscous fingering during immiscible displacement. Their test results do not conform to any CDC. As can be seen from Figure 23[101], for the same model, the residual phase saturation does not correlate well with the capillary number. Larger Ca does not necessarily lead to a larger displacement efficiency or lower displacement efficiency. It appears that sweep efficiency is affected

by capillary number which provides a new idea for EOR. As Eq.(1) shows, the displacement efficiency and the sweep efficiency are two independent parameters. Probably this is caused by an incorrect calculation of the capillary number. Similarly, Zhao et al[100] reported very interesting results that are difficult to explain by MiCa. Their typical test results are shown in Figure 24[112]. It is interesting that they do not adopt the definition of Ca from Eq.(3), although the contact angle can be well fixed. The residual phase saturation is not well correlated with MiCa. Their tests showed the importance of wettability on flow behavior. These results cannot be well explained by viscous fingering or capillary finger as proposed by Lenormand et al[86]. Both studies verified the atypical connection of sweep efficiency or displacement efficiency with Ca. For these special models, the displacement efficiency may also be sweep efficiency.

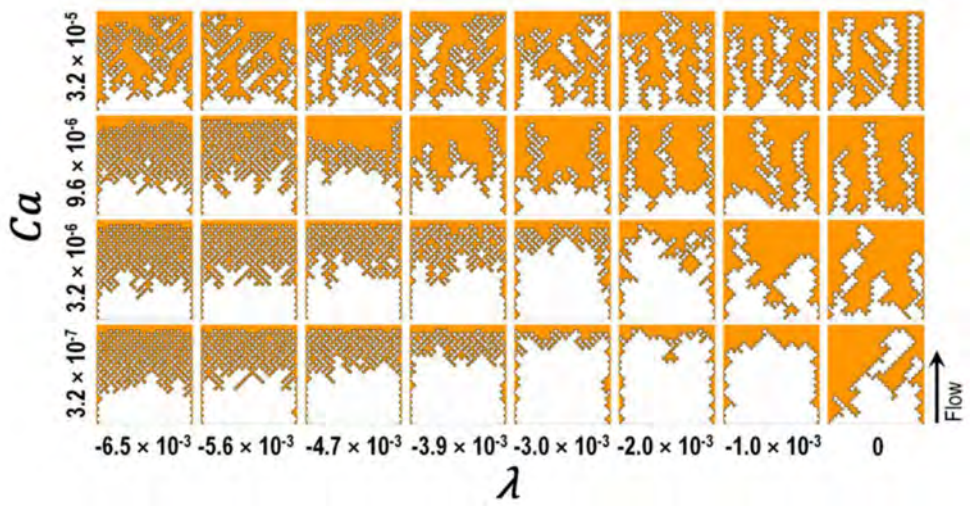

Figure 23—Sweep efficiency correlation with MiCa[101]

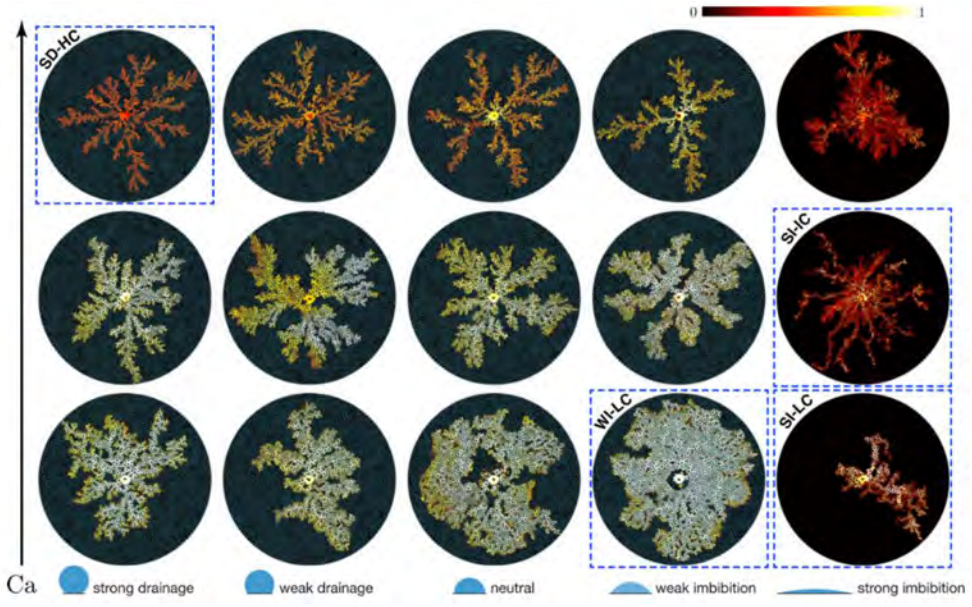

Figure 24—Sweep efficiency correlation with Ca and wettability[112]

How to account for these results by MaCa remains to be further investigated. Perhaps, these phenomena are caused by force balance which involves gravity, capillary force and viscous force. Recently, many researchers reported studies[120–124] on moderate IFT reduction by nanofluids can significantly increase EOR. This is also not consistent with classic capillary number theory in which ultra-low IFT is a necessary

condition. This can be explained by MaCa because IFT is not a direct parameter and not so important as previous believed. What is more important is the relative force balance in porous media. Ultra-low IFT is a special requirement only for capillary trapped ganglia remobilization. For much well-connected oil ganglia, a moderate IFT reduction is enough to cause proper wettability change and emulsification which contributes significantly to EOR.

Discussion

For many core flooding tests in EOR, the cores are placed horizontally in which the influence of gravity can be neglected because the gravity orientation is vertical to flow direction. This is based on the assumption that the viscous force is not affected by the orthogonal gravity. However, this may not always be true when the relative magnitude of gravity to capillary force and viscous force is large. Besides, gravity may affect viscous force because pores in microscopic scale are not all and completely horizontal. In particular, different from the common assumption of horizontal orientation, permeability is actually anisotropic[50,51,54]. When the three forces orientation are the same and their magnitude is comparable, it has significant meaning to combine them. Otherwise, it is less meaningful. Hence, trapped number[27] should be carefully used. When cores are placed vertically, the gravity force can play an important role in displacement. The gravity affected flow is shown in Figure 25. Gravity force can stabilize flow which is viscous fingering or capillary fingering. A surfactant flooding [82] without addition of polymer reported very low ROS and high oil recovery typical only possible in presence of polymer to help control mobility. Similarly, the low ROS in vertical core polymer flooding[80,81] is also caused by gravity stabilization effect. Figure 24 shows the effect of gravity on flow. The gravity effect in both microscopic and macroscopic scale has been discussed in detail[59]. The gravity effect on flow and oil recovery is well studied by laboratory tests[125]. In practice, gravity plays an important role in thick layer reservoir and very viscous oil recovery like steam-assisted gravity drainage (SAGD).

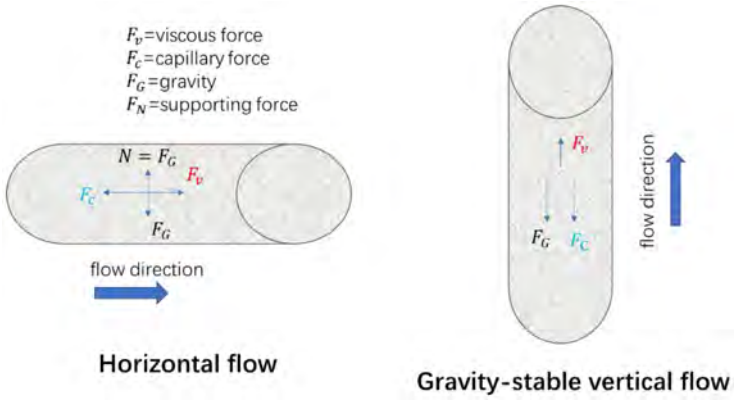

Figure 25—Gravity effect on flow

Another problem associated with the MiCa is the ultra-low IFT duration and working distance. Most Ca regarding IFT used a fixed value of IFT, this is possible for homogeneous models[26,86,100,101] and large slug of surfactants, however, ultra-low IFT can only last for a short distance in core or reservoirs. Thus the Ca values in many publications are too high for the IFT used. Another problem is that capillary force is a two-phase issue. When oil flows in the manner of connected pathway, there is low, or even no capillary force. The capillary number thus can be very large. This can be explained by MeCa, because even MiCa is very small, MeCa can be much larger since connected ganglia can be large compared to the average pore size. Besides, a large parameter of connected ganglia length makes it possible to bear a large pressure gradient. In a connected pathway with ganglia, no capillary force exists thus flow is easier. This process is observed[7]. Macroscopic parameters like relative permeability can only be used in MiCa when the pores are uniform

which form uniform capillary. Another important issue is the wettability which can be either microscopic and macroscopic. Recent studies showed that wettability has heterogeneous distribution[126–128] and is thus also scale dependent.

EOR application

As shown in Eq.(1), oil recovery involves both microscopic displacement efficiency and macroscopic sweep efficiency[1,2]. The current EOR theory is based on the classic Ca (MiCa) and CDCs. Classic CDCs imply that the IFT needs to be reduced to ultra-low and that the largest MiCa leads to the maximal oil recovery. The basic idea in chemical EOR is to reduce the IFT to ultra-low, and/or to increase brine viscosity to the largest extent. Recent studies[80,129] indicate that for polymer flooding higher MiCa does not necessarily make lower ROS. Other laboratory tests also indicate that optimal recovery is not always associated to the highest MiCa[12]. Although lots of CDC are based on MiCa experiments, many studies showed contradictory results. Increasing the displacing phase viscosity has the same contribution as reducing IFT if the MiCa is the same. However, many recent studies indicate that this is not practical. According to MaCa theory, the larger the value of MaCa, the larger the possibility to obtain a high oil recovery. The dynamic force balance in porous media is the most determing factor for EOR. Not realizing the importance of the dynamic change of moving and resistive forces, may lead to misinterpretions of experimental results. For instance, the ROS changed with MiCa during polymer flooding may have more to do with the gravity than the viscoelasticity of HPAM[80,81]. Latest updates of high concentration polymer flooding in Daqing indicate that it is not widely used [130] even after many years' large field tests and enthusiasm. This may discourage attemps to use polymer viscoelasticity effects for reducing ROS as believed by many researchers. There is no direct connection between IFT and ROS. As for surfactant flooding, ultra-low IFT is not the basic requirement. For polymer flooding, highest viscosity is not advised and for viscous oil, the required optimum polymer viscosity may be much lower than the unity mobility ratio requirement. This is especially important for low and high permeability formation. Another overlooked important parameter in EOR is interfacial viscoelastivity[114–119]. This parameter is not refleced in classic capillary number, while its correlation with macroscopic capillary parameters like saturation and capillary breakthrough pressure remains to be further investigated. Thus, the chemical EOR, which is based on classical CDC and MiCa theory needs to be improved.

The following studies are advised:

1. Recheck the wide belief that reducing the IFT to ultra-low is required in surfactant EOR.
2. Recheck the conclusion that HPAM can reduce the ROS significantly.
3. Investigate the connection between displacement efficiency and sweep efficiency.
4. Reexamine the importance of gravity in EOR.
5. Improve the numerical simulations in chemical EOR.

Conclusions

1. Current EOR theory is based on two important concepts: displacement efficiency and sweep efficiency, which are largely dependent on capillary number and mobility ratio respectively. Although sweep efficiency is generally deemed as a macroscopic concept, and displacement efficiency is regarded as microscopic, the distinction and connection between them is of great importance both in theory and practice.
2. The capillary number is well-accepted to reflect relative magnitude of driving force to resistance force. However, accurate characterization of these forces is scale-dependent.
3. 33 different Ca scaling groups have been summarized. These Cas can reflect some two-phase flow tests on certain given conditions.

4. The most widely used classic capillary number definition in EOR is proven microscopic in nature and is based on a contradictory assumption which has been overlooked for a long time. The macroscopic capillary number (MaCa) appears more reasonable than the microscopic capillary number (MiCa).
5. A concept of mesoscopic capillary number (MeCa) has been proposed as a connection between MiCa and MaCa.
6. CDC based on a classic microscopic Ca leads to the idea of reducing IFT to ultra-low to get a maximum displacement efficiency. This doctrine to reduce the IFT to ultra-low IFT has a wide application in chemical EOR.
7. Some recent laboratory tests and field tests indicate that the contribution of reducing IFT has been overestimated. This complex phenomenon cannot be well explained by classic microscopic Ca but are quite reasonable in macroscopic Ca circumstances.
8. As for chemical flooding, the importance of increasing displacing phase viscosity is much larger than reducing IFT for both heavy and light oil reservoir. Ultra-low IFT is not only unnecessary but also insufficient for a maximum recovery for most reservoir conditions according to force balance analysis based on macroscopic Ca. Inferfacial viscoelasticity plays an important role in EOR.
9. The MaCa is helpful to realize the importance of gravity on EOR due to the gravity effect the dynamic force balance in many complex heterogeneous reservoirs.
10. CDC based on macroscopic Ca calls for a new screening pattern for chemical EOR.

Acknowledgement

The authors wish to express their appreciation for the funding provided China Natural Science Foundation (51834005,51874320) the China Scholarship Council (201806440187) and Deutscher Akademischer Austauschdienst (91737128). The authors thank Johannes Hauskrecht and Tillmann Kleiner for comments on the manuscript.

Terminology

EOR = enhance oil recovery
Ca = capillary number
ROS = residual oil saturation
CDC = capillary desaturation curve
HPAM = partially hydrolyzed polyacrylamide
ASP = alkali-surfactant-polymer
SP = surfactant-polymer
E_D = sweep efficiency
E_v = displacement efficiency
Cac = critical capillary number
IFT = interfacial tension
v = velocity of displacing phase.
v_i = phase i Darcy velocity.
u = Darcy velocity in porous media p=viscosity of displacing phase
μ = oil viscosity.
μ_w = water viscosity.
μ_i = phase i viscosity
λ_w = water mobility
λ_w = oil mobility
θ = contact angle at boundary
σ = interfacial tension (IFT)

$\sigma_{0\text{-}w}$ = interfacial tension between oil and water phase.
L = length in direction of macroscopic flow.
D = average pore diameter
$\overline{D}$ = median pore diameter.
$\overline{De}$ = mean pore entry diameter
b_c = minimax width of the capillary
ψ = geometrical factor for curvature of front and back of trapped oil mass.
N_{Le} = Leverett number.
Z_{imb} = curvature correction factor for imbibition
f = dimensionless multipore oil filament length to radius ratio
r_n = pore neck radius.
μ_i = velocity of phase i.
μ^w = wetting phase viscosity.
K = permeability
$K_i^r(S)$ = phase i relative permeability curve function at saturation S
K_{rw} = relative pemeability to water.
K^{rw} = relative permeability to wetting phase, m^2
K_w = permeability to water
K_a = permeability to air
P_b = breakthrough pressure from capillary pressure curve.
P_c = capillary pressure.
P^c = average capillary pressure calculated
$P_c\ (S)$ = capillary pressure at saturation S.
ΔP = pressure drop over distance L.
l^{cl} = average cluster length.
l_{co} = connected oil ganglia
$\overrightarrow{l}$ = mean length of an oil ganlion
ϕ = porosity
r_p = radius of a pore
r_1, r_2 = D pore radius
X_c = width of pore-throat
∇P = pressure gradient
L_g = length of a ganglion
k_f = fracture permeability
d_b = pore-body aperture
d_t = pore-throat aperture
a = pore-throat diameter of micromodel
b = depth of the micromodel
V^{Darcy} = Darcy velocity
SAGD = steam-assisted gravity drainage

References

1. Green DW, Willhite GP. *Enhanced Oil Recovery.* 2nd ed. Richardson: Society of Petroleum Engineers; 2018.
2. Lake LW, Johns R, Rossen B, Pope G. *Fundamentals of Enhanced Oil Recovery.* 2nd ed. Richardson, Texas: Society of Petroleum Engineers; 2014.

3. Sheng JJ. *Enhanced Oil Recovery Field Case Studies.* 1st ed. London: Gulf Professional Publishing; 2013. https://doi.org/10.1016/B978-0-12-386545-8.00022-1.
4. Sheng JJ. *Modern Chemical Enhanced Oil Recovery.* Oxford: Gulf Professional Publishing; 2011.
5. Taber JJ. Research on Enhanced Oil Recovery: Past, Present and Future. *Pure Appl Chem* 1980;**52**:1323–47.
6. Bear J. *Dynamics of Fluids in Porous Media.* 1st ed. New York: Reprint of the American Elsevier Publishing Company; 1972.
7. Rucker M, Berg S, Armstrong RT, Georgiadis A, Ott H, Schwing A, et al From connected pathway flow to ganglion dynamics. *Geophys Res Lett* 2015;**42**:3888–94. https://doi.org/10.1002/2015GL064007.
8. Gogarty WB. Status of Surfactant or Micellar Methods. *J Pet Technol* 1976;**28**:93–102. SPE-5559-PA.
9. Thomas S, Farouq Ali SM. Micellar-Polymer Flooding: Status and Recent Advances. *J Can Pet Technol* 1992;**31**:53–60. https://doi.org/10.2118/92-08-05.
10. Guo H, Li Y, Gu Y, Wang F. Comparison of Strong Alkali and Weak Alkali ASP Flooding Pilot Tests in Daqing Oilfield. *SPE Prod Oper* 2018;**22**:353–62.
11. Guo H, Li Y, Kong D, Ma R, Li B, Wang F. Lessons Learned from Alkali-Surfactant-Polymer(ASP) Flooding Field Tests in China. *SPE Reserv Eval Eng* 2019;**22**:78–99. https://doi.org/doi.org/10.2118/186036-PA.
12. Guo H, Ma D, Wang H, Wang F, Gu Y, Yu Z, et al Proper Use of Capillary Number in Chemical Flooding. *J Chem* 2017;**2017**:1–19.
13. Guo H, Dou M, Hanqing W, Wang F, Yuanyuan G, Yu Z, et al Review of Capillary Number in Chemical Enhanced Oil Recovery. *SPE Kuwait Oil Gas Show Conf* 2015. https://doi.org/10.2118/175172-MS.
14. Zhu Y, Hou Q, Jian G, Ma D, Wang Z. Current development and application of chemical combination flooding technique. *Pet Explor Dev* 2013;**40**:96–103. https://doi.org/10.1016/S1876-3804(13)60009-9.
15. Zhu Y, Zhang Y, Niu J, Liu W, Hou Q. The research progress in the alkali-free surfactant-polymer combination flooding technique. *Pet Explor Dev* 2012;**39**:371–6. https://doi.org/10.1016/S1876-3804(12)60053-6.
16. Liao G, Wang Q, Wang H, Liu W, Wang Z. Chemical Flooding Development Status and Prospect. *Acta Pet Sin (Shiyou Xuebao)* 2017;**38**:196–207.
17. Liu W, Luo L, Liao G, Zuo L, Wei Y, Jiang W. Experimental study on the mechanism of enhancing oil recovery by polymer-surfactant binary flooding. *Shiyou Kantan Yu Kaifa/Petroleum Explor Dev* 2017;**44**:600–7. https://doi.org/10.11698/PED.2017.04.13.
18. Larson RG, Davis HT, Scriven LE. Displacement of residual nonwetting fluid from porous media. *Chem Eng Sci* 1981;**36**:75–85. https://doi.org/10.1016/0009-2509(81)80049-8.
19. Moore TF, Slobod RL. Displacement of Oil by Water-Effect of Wettability, Rate, and Viscosity on Recovery. SPE- 502-G. *Fall Meet. Pet. Branch AIME*, 1955, p. 16. https://doi.org/10.2118/502-G.
20. Reed LR, Healy RN. Some Physicochemical Aspects of Microemulsion Flooding: A Review. AIChE Symp. Improv. Oil Recover. by Surfactant Polym. Flooding, Kansas City, Kansas, 12-14 April, 1977, p. 383–437. https://doi.org/10.1016/0030-4220(77)90406-6.
21. Fulcher, Richard Alfred J. The Effect of the Capillary Number and Its Constituents on Two-Phase Relative Permeabilities. *The Pennsylvania State University*, 1982.

22. Arriola A, Willhite GP, Green DW. Trapping of Oil Drops in a Noncircular Pore Throat and Mobilization Upon Contact With a Surfactant. *SPE-9404-PA. Soc Pet Eng J* 1983;**23**:99–114. https://doi.org/10.2118/9404-pa.
23. Chatzis I, Morrow N. Correlation of Capillary Number Relationships for Sandstone. *Soc Pet Eng J* 1984;**24**:555–62. https://doi.org/10.2118/10114-PA.
24. Morrow N, Lim H, Ward J. Effect of Crude-Oil-Induced Wettability Changes on Oil Recovery. *SPE Form Eval* 1986;**1**:89–103. https://doi.org/10.2118/13215-PA.
25. Chatzis I, Kuntamukkula MS, Morrow NR. Effect of Capillary Number on the Microstructure of Residual Oil in Strongly Water-Wet Sandstones. SPE-13213-PA. *SPE Reserv Eng* 1988;**3**:903–12. https://doi.org/10.2118/13213-PA.
26. Morrow NR, Chatzis I, Taber JJ. Entrapment and Mobilization of Residual Oil in Bead Packs. *SPE Reserv Eng* 1988;**3**:927–34. https://doi.org/10.2118/14423-PA.
27. Youssef S, Peysson Y, Bauer D, Vizika O, Energie IFP, Bois-preau D. Capillary Desaturation Curve Prediction Using 3D Microtomography Images. Int. Symp. Soc. Core Anal. held St. John's Newfoundl. Labrador, Canada, 1621 August, 2015, 2015, p. 1–12.
28. Delshad M, Fathi Najafabadi N, Anderson G, Pope G, Sepehrnoori K. Modeling Wettability Alteration By Surfactants in Naturally Fractured Reservoirs. *SPE Reserv Eval Eng* 2009;**12**:361–70. https://doi.org/10.2118/100081-PA.
29. Humphry KJ, Suijkerbuijk BMJM, Linde H a Van Der, Pieterse SGJ, Masalmeh SK. *Impact of Wettability on Residual Oil Saturation and Capillary Desaturation Curves* 2013;**55**:1–11.
30. AlQuaimi BI, Rossen WR. Capillary Desaturation Curve for Residual Nonwetting Phase in Natural Fractures. *SPE J* 2018;**23**:788–802. https://doi.org/10.2118/189448-PA.
31. Chatzis I, Morrow NR. Correlation of Capillary Number Relationships for Sandstone. SPE-101 14-PA. *Soc Pet Eng J* 1984;**24**:555–62. https://doi.org/10.2118/10114-PA.
32. Leverett MC. Capillary Behavior in Porous Solids. SPE-941152-G. *Trans AIME* 1941;**142**:152–96. https://doi.org/10.1515/crll.1958.200.129.
33. Saffman PG, Taylor GI. The penetration of a fluid into a porous medium or Hele-Shaw cell containing a more viscous liquid. *Proc R Soc Lond A* 1958;245.
34. Taber J. Dynamic and Static Forces Required To Remove a Discontinuous Oil Phase from Porous Media Containing Both Oil and Water. SPE-2098-PA. *Soc Pet Eng J* 1969;**9**:3–12.
35. Foster WR. A Low-Tension Waterflooding Process. SPE-3803-PA. *J Pet Technol* 1973;**25**:205–10.
36. Lefebvre du Prey EJ. Factors Affecting Liquid-Liquid Relative Permeabilities of a Consolidated Porous Medium. SPE-3039-PA. *Soc Pet Eng J* 1973;**13**:39–47. https://doi.org/10.2118/3039-PA.
37. Melrose JC, Brandner CF. Role of Capillary Forces in Determining Microscopic Displacement Efficiency for Oil Recovery by Waterflooding. *J Can Pet Technol* 1974;**13**:54–62. https://doi.org/dx.doi.org/10.2118/74-04-05.
38. Ehrlich R, Hasiba HH, Raimondi P. Alkaline Waterflooding for Wettability Alteration-Evaluating a Potential Field Application. *J Pet Technol* 1974;**26**:1335–43. https://doi.org/10.2118/4905-PA.
39. Abrams A. The Influence of Fluid Viscosity, Interfacial Tension, and Flow Velocity on Residual Oil Saturation Left by Waterflood. *Soc Pet Eng J* 1975;**15**:437–47. https://doi.org/10.2118/5050-PA.
40. Dullien FA., MacDonald IF. Correlating Tertiary Oil Recovery in Water-Wet Systems. SPE-5457-PA. *Soc Pet Eng J* 1976;**16**:7–9.
41. Stegemeier GL. Mechanisms of Entrapment and Mobilization of Oil in Porous Media. *Improv. Oil Recover. by Surfactant Polym. Flooding*, New York City: Academic Press. Inc; 1977, p. 55–91. https://doi.org/10.1016/B978-0-12-641750-0.50006-2.

42. Oh SG, Slattery JC. SPE-5992-PA. Interfacial Tension Required for Significant Displacement of Residual Oil. *Soc Pet Eng J* 1979;**19**:83=96.
43. Jiang Y. Prediction of the Relationship Between Capilary Number and Residual Oil Saturation. *Pet Geol Oilf Dev Daqing(PGODD)* 1987;**6**:63–6.
44. Hilfer R. Transport and Relaxation Phenomena in Porous Media. *Adv. Chem. Phys.*, vol. **92**, 1996, p. 299–424.
45. Hughes RG, Blunt MJ. Network modeling of multiphase flow in fracture. *Adv Water Resour* 2001;**24**:409–21. https://doi.org/10.1016/S0309-1708(00)00064-6.
46. Armstrong RT, Georgiadis A, Ott H, Klemin D, Berg S. Critical capillary number: Desaturation studied with fast X- ray computed microtomography. *Geophys Res Lett* 2014;**41**:55–60. https://doi.org/10.1002/2013GL058075.
47. Hilfer R, Armstrong RT, Berg S, Georgiadis A, Ott H. Capillary saturation and desaturation. *Phys Rev E* 2015;**92**:1–11. https://doi.org/10.1103/PhysRevE.92.063023.
48. Doorwar S, Mohanty KK. Viscous-fingering function for unstable immiscible flows. *SPE J* 2017;**22**:19–3 1.SPE-173290-PA.
49. Chang C, Kneafsey TJ, Zhou Q, Oostrom M, Ju Y. Scaling the impacts of pore-scale characteristics on unstable supercritical CO2-water drainage using a complete capillary number. *Int J Greenh Gas Control* 2019;**86**:11–21. https://doi.org/10.1016/j.ijggc.2019.04.010.
50. Hilfer R. Macroscopic equations of motion for two-phase flow in porous media. *Phys Rev E* 1998;**58**:2090–6. https://doi.org/10.1103/PhysRevE.58.2090.
51. Anton L, Hilfer R. Trapping and mobilization of residual fluid during capillary desaturation in porous media. *Phys Rev E* 1999;**59**:6819–23. https://doi.org/10.1103/PhysRevE.59.6819.
52. Biswal B, Hilfer R. Microstructure analysis of reconstructed porous media. *Physica A* 1999;**266**:307–11. https://doi.org/10.1016/S0378-4371(98)00607-4.
53. Hilfer R, Besserer H. Macroscopic two-phase flow in porous media. *Phys B* 2000;**279**:125–9. https://doi.org/10.1016/S0921-4526(99)00694-8.
54. Hilfer R. Review on scale dependent characterization of the microstructure of porous media. *Transp Porous Media* 2002;**46**:373–90. https://doi.org/10.1023/A:1015014302642.
55. Pickup GE, Hern CY. The development of appropriate upscaling procedures. *Transp Porous Media* 2002;**46**:119–38. https://doi.org/10.1023/A:1015055515059.
56. Hilfer R. Capillary pressure, hysteresis and residual saturation in porous media. *Physica A* 2006;**359**:119–28. https://doi.org/10.1016/j.physa.2005.05.086.
57. Hilfer R. Macroscopic capillarity without a constitutive capillary pressure function. *Physica A* 2006;**371**:209–25. https://doi.org/10.1016/j.physa.2006.04.051.
58. Hilfer R. Macroscopic capillarity and hysteresis for flow in porous media. *Phys Rev E* 2006;**73**:1–9. https://doi.org/10.1103/PhysRevE.73.016307.
59. Hilfer R, oren PE. Dimensional analysis of pore scale and field scale immiscible displacement. *Transp Porous Media* 1996;**22**:53–72. https://doi.org/10.1007/BF00974311.
60. Yeganeh M, Hegner J, Lewandowski E, Mohan A, Lake LW, Cherney D, et al Capillary Desaturation Curve Fundamentals. SPE Improv. Oil Recover. Conf., 2016, p. 14. https://doi.org/10.2118/179574-MS.
61. Han M, Alsofi A, Fuseni A, Zhou X, Hassan S, Aramco S. Devopment of Chemical EOR Formulations for a High Temperature and High Salinity Carbonate Reservoir. IPTC-17084. Int. Pet. Technol. Conf. held Beijing, 2013.
62. Gupta SP, Trushenski SP. Micellar Flooding - Compositional Effects on Oil Displacement. *Soc Pet Eng J* 1979;**19**:116–28.

63. Lenormand R, Zarcone C. Physics of Blob Displacement in a Two-Dimensional Porous Medium. *SPE Form Eval* 1988;**3**:271–5. https://doi.org/10.2118/14882-PA.
64. Mohanty K. Multiphase Flow in Porous Media: III. Oil Mobilization, Transverse Dispersion, and Wettability. SPE-12127-MS. SPE Annu. Tech. Conf. Exhib., 1983. https://doi.org/10.2523/12127-MS.
65. Andrew CE, Fjelde I, Abeysinghe K, Lohne A. Effect of interfacial tension on water/oil relative permeability and remaining saturation with consideration of capillary pressure. SPE-143028-MS. SPE Eur. Conf. Exhib. held Vienna, Austria, 2011. https://doi.org/10.2118/143028-MS.
66. Abeysinghe KP, Fjelde I, Lohne A. Dependency of remaining oil saturation on wettability and capillary number. *SPE Saudi Arab Sect Tech Symp Exhib* 2012. https://doi.org/10.2118/160883-MS.
67. Guo H, Yiqiang L, Ruicheng M, Fuyong W, Zhang S. Evaluation of Three Large Scale ASP Flooding Field Test. 19th Eur. Symp. Improv. Oil Recover. 24-27 April 2017, Stavanger, Norw., 2017, p. 1–11.
68. Zhang H, Dong M, Zhao S. Which one is more important in chemical flooding for enhanced court heavy oil recovery, lowering interfacial tension or reducing water mobility? *Energy and Fuels* 2010;**24**:1829–36. https://doi.org/10.1021/ef901310v.
69. Gao S, Peng S, Han P, Chen G, Liu H, Yan W, et al Enhanced oil recovery test based on wells and stations utilization to reduce cost after polymer flooding. SPE Middle East Oil Gas Show Conf. MEOS, 2019, p. 1–9. https://doi.org/10.2118/194752-ms.
70. Hou J, Liu Z, Zhang S, Yue X, Yang J. The role of viscoelasticity of alkali/surfactant/polymer solutions in enhanced oil recovery. *J Pet Sci Eng* 2005;**47**:219–35. https://doi.org/10.1016/j.petrol.2005.04.001.
71. Shen P, Wang J, Yuan S, Zhong T, Jia X. Study of enhanced-oil-recovery mechanism of alkali/surfactant/polymer flooding in porous media from experiments. *SPE J* 2009;**14**:237–44. https://doi.org/10.2118/126128-PA.
72. Wang Y, Zhao F, Bai B, Zhang J, Xiang W, Li X, et al Optimized Surfactant IFT and Polymer Viscosity for Surfactant- Polymer Flooding in Heterogeneous Formations. SPE Improv. Oil Recover. Symp. 24-28 April. Tulsa, Oklahoma, USA, 2010, p. 1–11.
73. Qi LQ, Liu ZZ, Yang CZ, Yin YJ, Hou JR, Zhang J, et al Supplement and optimization of classical capillary number experimental curve for enhanced oil recovery by combination flooding. *Sci China Technol Sci* 2014;**57**:2190–203. https://doi.org/10.1007/s11431-014-5666-2.
74. Wang D, Wang G, Wu W, Xia H, Yin H. The influence of viscoelasticity on displacement efficiency -From micro- To macroscale. *SPE Annu Tech Conf Exhib* 2007;**1**:304–13. https://doi.org/10.2523/109016-ms.
75. Azad MS, Trivedi JJ. Quantification of the Viscoelastic Effects During Polymer Flooding: A Critical Review. *SPE J* 2019:1–27. https://doi.org/10.2118/195687-pa.
76. Azad MS, Trivedi JJ. Does Polymer's Viscoelasticity Influence Heavy-Oil Sweep Efficiency and Injectivity at 1 ft / D ? SPE-193771-PA. *SPE Reserv Eval Eng* 2019.
77. Wang D, Jiang Y, Wang Y, Gong X, Wang G. Viscous-Elastic Polymer Fluids Rheology and Its Effect Upon Production Equipment. SPE-77496-PA. *SPE Prod Facil* 2004;**19**:209–16. https://doi.org/10.2118/77496-PA.
78. Wang D, Cheng J, Yang Q, Gong W, Li Q. Viscous-elastic polymer can increase microscale displacement efficiency in cores. SPE-63227-MS. SPE Annu. Tech. Conf. Exhib., 2000. https://doi.org/10.2523/63227-ms.
79. Needham RB, Doe PH. Polymer Flooding Review. *J Pet Technol* 1987;**39**:1503–7. SPE-17140-PA.

80. Qi P, Ehrenfried DH, Koh H, Balhoff MT. Reduction of residual oil saturation in sandstone cores by use of viscoelastic polymers. *SPE J* 2017;**22**:447–58. https://doi.org/10.2118/179689-PA.
81. Erincik MZ, Qi P, Balhoff MT, Pope GA. New method to reduce residual oil saturation by polymer flooding. *SPE J* 2018;**23**:1944–56. https://doi.org/10.2118/187230-pa.
82. Lu J, Pope GA. Optimization of Gravity-Stable Surfactant Flooding. *SPE J* 2017;**22**:480–93.
83. Mai A, Bryan J, Goodarzi N, Kantzas A. Insights into non-thermal recovery of heavy oil. *J Can Pet Technol* 2009;**48**:27–35. https://doi.org/10.2118/09-03-27.
84. Mai A, Kantzas A. Heavy Oil Waterflooding: Effects of Flow Rate and Oil Viscosity. *J Can Pet Technol* 2009;**48**:42–51.
85. Andrew EC, Fjelde I, Abeysinghe K, Lohne A. Effect of Interfacial Tension on Water/Oil Relative Permeability on the Basis of History Matching to Coreflood Data. *SPE Reserv Eval Eng* 2014;**17**:37–48. https://doi.org/10.2118/143028-PA.
86. Lenormand R, Touboul E, Zarcone C. Numerical models and experiments on immiscible displacements in porous media. *J Fluid Mech* 1988;**189**:165–87. https://doi.org/10.1017/S0022112088000953.
87. McDougall SR, Sorbie KS. Combined effect of capillary and viscous forces on waterflood displacement efficiency in finely laminated porous media. *SPE Annu Tech Conf Exhib* 1993;Sigma:563–78. https://doi.org/10.2523/26659-ms.
88. Scheneider M. *Nonlinear Finite Volume Schemes for Complex Flow Processes and Challenging Grids.* University of Stuttgart, 2019.
89. Georgiadis A, Berg S, Makurat A, Maitland G, Ott H. Pore-scale micro-computed-tomography imaging: Nonwetting- phase cluster-size distribution during drainage and imbibition. *Phys Rev E* 2013;**88**:1–9. https://doi.org/10.1103/PhysRevE.88.033002.
90. Hilfer R, Lemmer A. Differential porosimetry and permeametry for random porous media. *Phys Rev E - Stat Nonlinear, Soft Matter Phys* 2015;**92**:29–32. https://doi.org/10.1103/PhysRevE.92.013305.
91. Hilfer R, Biswal B, Mattutis HG, Janke W. Multicanonical simulations of the tails of the order-parameter distribution of the two-dimensional Ising model. *Comput Phys Commun* 2005;**169**:230–3. https://doi.org/10.1016/j.cpc.2005.03.053.
92. Hilfer R, Seybold HJ. Computation of the generalized Mittag-Leffler function and its inverse in the complex plane. *Integr Transform Spec Funct* 2006;**17**:637–52. https://doi.org/10.1080/10652460600725341.
93. Aghaei A, Piri M. Direct pore-to-core up-scaling of displacement processes: Dynamic pore network modeling and experimentation. *J Hydrol* 2015;**522**:488–509. https://doi.org/10.1016/j.jhydrol.2015.01.004.
94. Mattila K, Puurtinen T, Hyvaluoma J, Surmas R, Myllys M, Turpeinen T, et al A prospect for computing in porous materials research: Very large fluid flow simulations. *J Comput Sci* 2016;**12**:62–76. https://doi.org/10.1016/j.jocs.2015.11.013.
95. Armstrong RT, McClure JE, Berill MA, Rucker M, Schluter S, Berg S. Flow regimes during immiscible displacement. *Petrophysics* 2017;**58**:10–8.
96. Biswal B, Manwart C, Hilfer R. Three-dimensional local porosity analysis of porous media. *Phys A Stat Mech Its Appl* 1998;**255**:221–41. https://doi.org/10.1016/S0378-4371(98)00111-3.
97. Morrow NR, Chatzis I, Taber JJ. Entrapment and Mobilization of Residulal Oil in Bead Packs. SPE-14423-PA. *SPE Reserv Eng* 1988;**3**:927–34.
98. Dullien F a. L. *Porous Media Fluid Transport and Pore Structure Second Edition.* 2nd ed. Academic Press. Inc; 1992. https://doi.org/10.1364/OL.39.005657.

99. Schluter S, Berg S, Rucker M, Armstrong RT, Vogel HJ, Hilfer R, et al Pore-scale displacement mechanisms as a source of hysteresis for two-phase flow in porous media. *Water Resour Res* 2016;**52**:2194–205. https://doi.org/10.1002/2015WR018254.
100. Zhao B, MacMinn CW, Juanes R. Wettability control on multiphase flow in patterned microfluidics. *Proc Natl Acad Sci U S A* 2016;**113**:10251–6. https://doi.org/10.1073/pnas.1603387113.
101. Rabbani HS, Or D, Liu Y, Lai CY, Lu NB, Datta SS, et al Suppressing viscous fingering in structured porous media. *Proc Natl Acad Sci U S A* 2018;**115**:4833–8. https://doi.org/10.1073/pnas.1800729115.
102. Roof JG. Snap-Off of Oil Droplets in Water- Wet Pores. *Soc Pet Eng J* 1970;**10**:85–90. SPE-2504-PA.
103. Hoyer P, Alvarado V, Carvalho MS. Snap-offin constricted capillary with elastic interface. *Phys Fluids* 2016;28. https://doi.org/10.1063/1.4939150.
104. Pak T, Butler IB, Geiger S, Van Dijke MIJ, Sorbie KS. Droplet fragmentation: 3D imaging of a previously unidentified pore-scale process during multiphase flow in porous media. *Proc Natl Acad Sci U S A* 2015;**112**:1947–52. https://doi.org/10.1073/pnas.1420202112.
105. Datta SS, Ramakrishnan TS, Weitz DA. Mobilization of a trapped non-wetting fluid from a three-dimensional porous medium. *Phys Fluids* 2014;26. https://doi.org/10.1063/1.4866641.
106. Berg S, Ott H, Klapp SA, Schwing A, Neiteler R, Brussee N, et al Real-time 3D imaging of Haines jumps in porous media flow. *Proc Natl Acad Sci U S A* 2013;**110**:3755–9. https://doi.org/10.1073/pnas.1221373110.
107. Armstrong RT, Berg S. Interfacial velocities and capillary pressure gradients during Haines jumps. *Phys Rev E* 2013;**88**:1–9. https://doi.org/10.1103/PhysRevE.88.043010.
108. Stegemeier GL. Relationship of Trapped Oil Saturation to Petrophysical Properties of Porous Media. *SPE Improv Oil Recover Symp* 1974. https://doi.org/10.2118/4754-MS.
109. Andrew M, Bijeljic B, Blunt MJ. Pore-scale contact angle measurements at reservoir conditions using X-ray microtomography. *Adv Water Resour* 2014;**68**:24–31. https://doi.org/10.1016/j.advwatres.2014.02.014.
110. Ruspini LC, Farokhpoor R, oren PE. Pore-scale modeling of capillary trapping in water-wet porous media: A new cooperative pore-body filling model. *Adv Water Resour* 2017;**108**:1–14. https://doi.org/10.1016/j.advwatres.2017.07.008.
111. Wilkinson D. Percolation effects in immiscible displacement. *Phys Rev A* 1986;**34**:1380–91.
112. Zhao B, MacMinn CW, Primkulov BK, Chen Y, Valocchi AJ, Zhao J, et al Comprehensive comparison of pore- scale models for multiphase flow in porous media. *Proc Natl Acad Sci U S A* 2019;**116**:13799–806. https://doi.org/10.1073/pnas.1901619116.
113. Guo H, Li Y, Wang F, Yu Z, Chen Z, Wang Y. ASP Flooding: Theory and Practice Progress in China. *J Chem* 2017;**2017**:1–32.
114. Slattery JC. Interfacial Effects in the Entrapment and Displacement of Residual Oil. *AICHE J* 1984;**20**:1145–53.
115. Bourgoyne AT, Caudle B.H., Kimbler O.K. Effect of interfacial films on the displacement of oil by water in porous media. SPE-3272-PA. *Soc Pet Eng J* 1972;**12**:60–8. https://doi.org/10.2118/3272-pa.
116. Cooke CE, Williams RE, Kolodzie PA. Oil Recovery By Alkaline Waterflooding. *J Pet Technol* 1974;**26**:1365–74. https://doi.org/10.2118/4739-PA.
117. Lakatos-Szabo J, Lakatos I. Effect of alkaline materials on interfacial rheological properties of oil-water systems. *Colloid Polym Sci* 1999;**277**:41–7. https://doi.org/10.1007/s003960050365.

118. Bidhendi MM, Garcia-Olvera G, Morin B, Oakey JS, Alvarado V. Interfacial viscoelasticity of crude oil/brine: An alternative enhanced-oil-recovery mechanism in smart waterflooding. SPE-169127-PA. *SPE J* 2018;**23**:803–18.
119. Alvarado V, Garcia-Olvera G, Hoyer P, Lehmann TE. Impact of polar components on crude oil-water interfacial film formation: A mechanisms for low-salinity water flooding. *SPE Annu Tech Conf Exhib* 2014; SPE-170807-MS.
120. Raj I, Qu M, Xiao L, Hou J, Li Y, Liang T, et al Ultralow concentration of molybdenum disulfide nanosheets for enhanced oil recovery. *Fuel* 2019;**251**:514–22. https://doi.org/10.1016/j.fuel.2019.04.078.
121. Luo D, Wang F, Zhu J, Cao F, Liu Y, Li X, et al Nanofluid of graphene-based amphiphilic Janus nanosheets for tertiary or enhanced oil recovery: High performance at low concentration. *Proc Natl Acad Sci U S A* 2016;**113**:7711–6. https://doi.org/10.1073/pnas.1608135113.
122. Radnia H, Rashidi A, Solaimany Nazar AR, Eskandari MM, Jalilian M. A novel nanofluid based on sulfonated graphene for enhanced oil recovery. *J Mol Liq* 2018;**271**:795–806. https://doi.org/10.1016/j.molliq.2018.09.070.
123. Rosestolato JCS, Perez-Gramatges A, Lachter ER, Nascimento RSV. Lipid nanostructures as surfactant carriers for enhanced oil recovery. *Fuel* 2019;**239**:403–12. https://doi.org/10.1016/j.fuel.2018.11.027.
124. Dai C, Huang Y, Lyu X, Li L, Sun Y, Zhao M, et al Solid-like film formed by nano-silica self-assembly at oil-water interface. *Chem Eng Sci* 2019;**195**:51–61. https://doi.org/10.1016/j.ces.2018.11.042.
125. Adebayo AR, Barri AA, Kamal MS. Residual saturation: An experimental study of effect of gravity and capillarity during vertical and horizontal flow. SPE-187998-MS. SPE Kingdom Saudi Arab. Annu. Tech. Symp. Exhib., 2017.
126. Berthet H, Hebert M, Barbouteau S, Andriamananjaona P, Rivenq R. Pore-scale insights on trapped oil during waterflooding of sandstone rocks of varying wettability states'. *Petrophysics* 2019;**60**:229–39. https://doi.org/10.30632/PJV60N2-2019a1.
127. Alpak FO, Zacharoudiou I, Berg S, Dietderich J, Saxena N. Direct simulation of pore-scale two-phase visco-capillary flow on large digital rock images using a phase-field lattice Boltzmann method on general-purpose graphics processing units. *Comput Geosci* 2019;**23**:849–80. https://doi.org/10.1007/s10596-019-9818-0.
128. Teklu TW, Alameri W, Kazemi H, Graves RM. Contact angle measurements on conventional and unconventional reservoir cores. Unconv. Resour. Technol. Conf. URTeC 2015, 2015, p. 1–17. https://doi.org/10.2118/178568-ms.
129. Seright RS. How Much Polymer Should Be Injected During a Polymer Flood? Review of Previous and Current Practices. *SPE J* 2017;**22**:11–3. https://doi.org/10.2118/179543-PA.
130. Wang D. Technical innovation greatly increase the recoverable reserve and ensure long- term high production of Daqing Oilfield. *Pet Geol Oilf Dev Daqing(PGOD)* 2019;**38**:8–17.